MALT 90
The Millimetre Astronomy Legacy Team 90 GHz Survey

James Jackson
Institute for Astrophysical Research
Boston University

Soul of High Mass Star Formation; 18 March 2015

Special Thanks

Friedrich Wyrowski,

Frédéric Schuller,

And the ATLASGAL team

For generously providing ATLASGAL 870 μm positions for our targets before publication:

(Contreras et al. 2013; Csengeri et al. 2014)

Collaborators (partial list)

Jill Rathborne	CSIRO
Jonathan Foster	Yale
Scott Whitaker	Boston University
Yanett Contreras	CSIRO
Andres Guzman	CfA and U. Chile
Ian Stephens	Boston University
Friedrich Wyrowski	MPIfR
Sadia Hoq	Boston University
Patricio Sanhueza	Boston University/NAOJ
Steve Longmore	Liverpool John Moores U.

$$\nabla \cdot \mathbf{E} = \frac{\rho}{\varepsilon_0}$$

$$\nabla \cdot \mathbf{B} = 0$$

$$\nabla \times \mathbf{E} = -\frac{\partial \mathbf{B}}{\partial t}$$

$$\nabla \times \mathbf{B} = \mu_0 \mathbf{J} + \mu_0 \varepsilon_0 \frac{\partial \mathbf{E}}{\partial t}$$

$$\nabla \cdot \mathbf{E} = \frac{\rho}{\varepsilon_0}$$

$$\nabla \cdot \mathbf{B} = 0$$

$$\nabla \times \mathbf{E} = -\frac{\partial \mathbf{B}}{\partial t}$$

$$\nabla \times \mathbf{B} = \mu_0 \mathbf{J} + \mu_0 \varepsilon_0 \frac{\partial \mathbf{E}}{\partial t}$$

Clumps forming High-Mass Stars

- What are their physical and chemical properties?
- What is their Galactic distribution?
- How do they evolve?

We need a statistical approach: SURVEYS

How do high-mass star-forming clumps evolve?

- Determine their evolutionary stage
- Measure their physical properties:
  - Distance
  - Kinematics
  - Chemistry
  - Temperature
  - Column Density

Advantages of Line Surveys over Continuum Surveys

- Velocity Information
  - Kinematics
  - Distances
  - Separation of Blended Sources
- Chemistry
- Gas vs. Dust

The evolutionary phases of high-mass star forming clumps

0.2 degrees

1.2 degrees

The "Nessie" Nebula
Jackson et al. 2010 ApJ Letters

Blue - 3.6μm, Green - 8μm, Red - 24μm

Image credit: NASA/JPL-Caltech/Univ. of Wisconsin

Pre-stellar

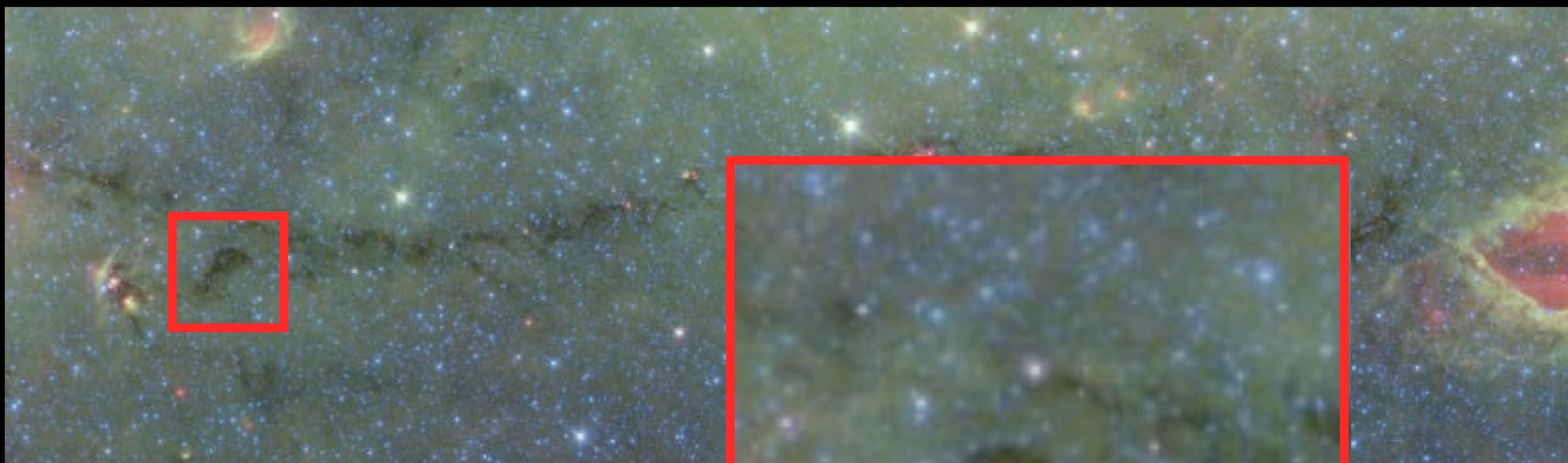

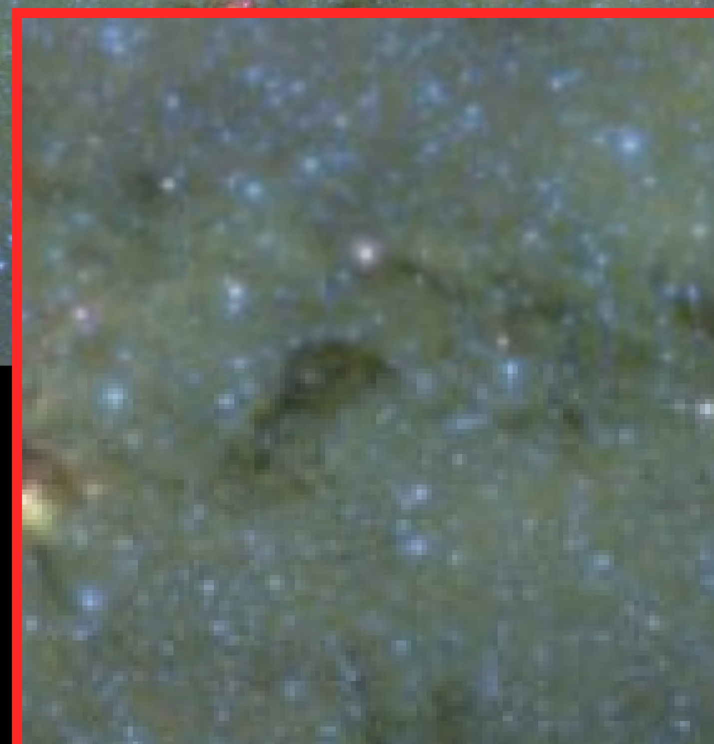

Early stage

Cold "quiescent" pre-stellar clump

Blue - 3.6μm, Green - 8μm, Red - 24μm

Image credit: NASA/JPL-Caltech/Univ. of Wisconsin

Protostellar

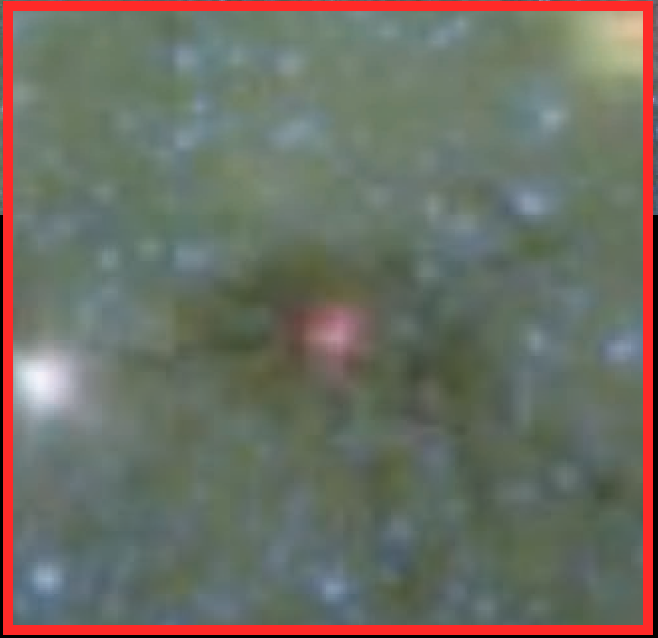

Intermediate stage

Protostellar clump

Blue - 3.6μm, Green - 8μm, Red - 24μm

Image credit: NASA/JPL-Caltech/Univ. of Wisconsin

H II region

Later stage

Stellar "H II region" clump

Blue - 3.6μm, Green - 8μm, Red - 24μm

Image credit: NASA/JPL-Caltech/Univ. of Wisconsin

Photodissociation Region (PDR)

Latest stage

Photodissociation region (PDR)

Blue - 3.6μm, Green - 8μm, Red - 24μm

Image credit: NASA/JPL-Caltech/Univ. of Wisconsin

Clump classification: *Spitzer* mid-IR

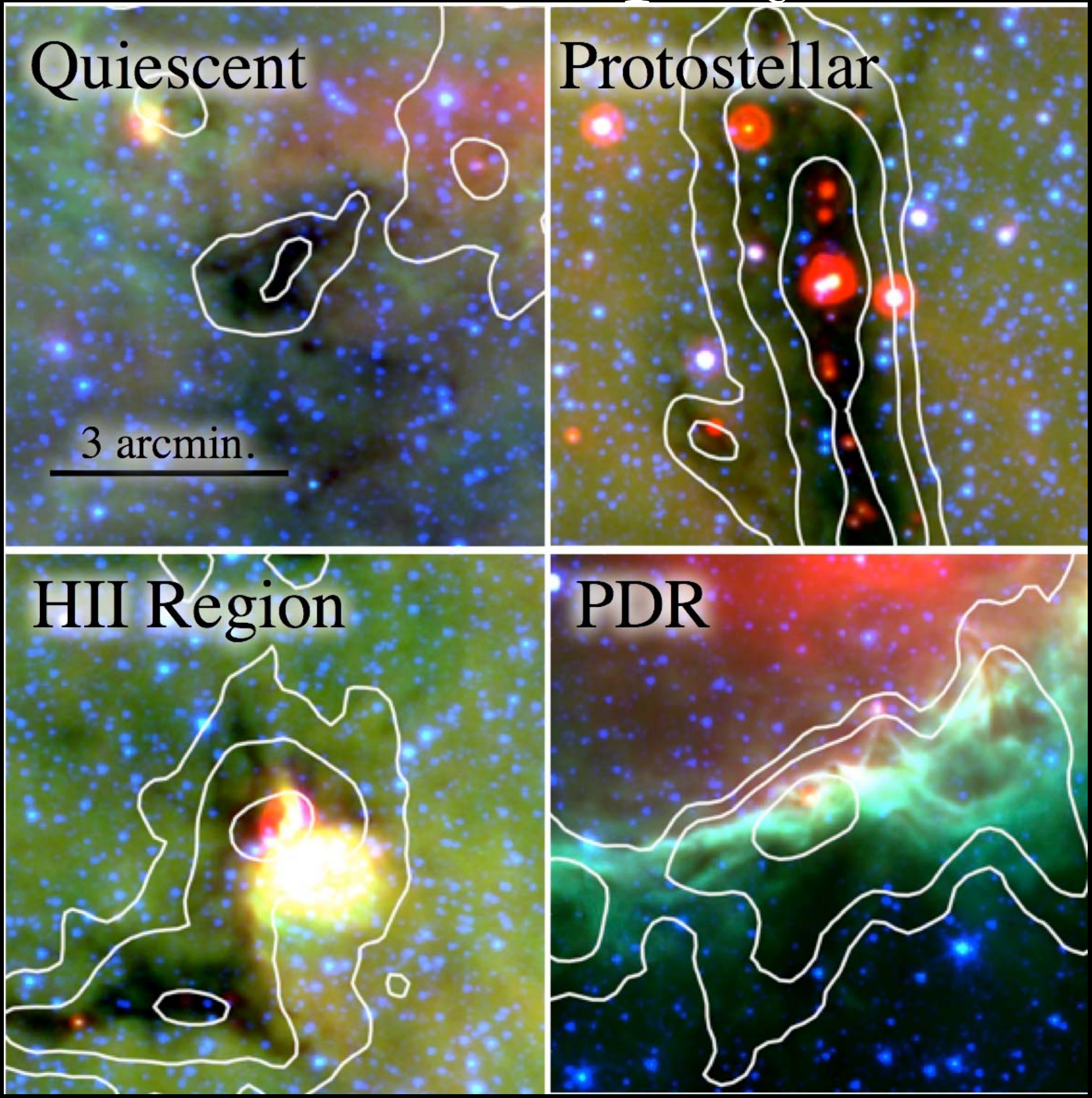

Blue 3.6 μm Green 8 μm, Red 24 μm Spitzer: GlIMPLSE/MIPSGAL Contours: ATLASGAL 870 μm

Dust Continuum Surveys

- ATLASGAL (870 um)
- HiGAL (70 to 500 μm)
- BGPS (1300 μm)
- MIPSGAL (24 μm)
- GLIMPSE (3 – 8 μm)

These surveys have identified thousands of molecular clumps.

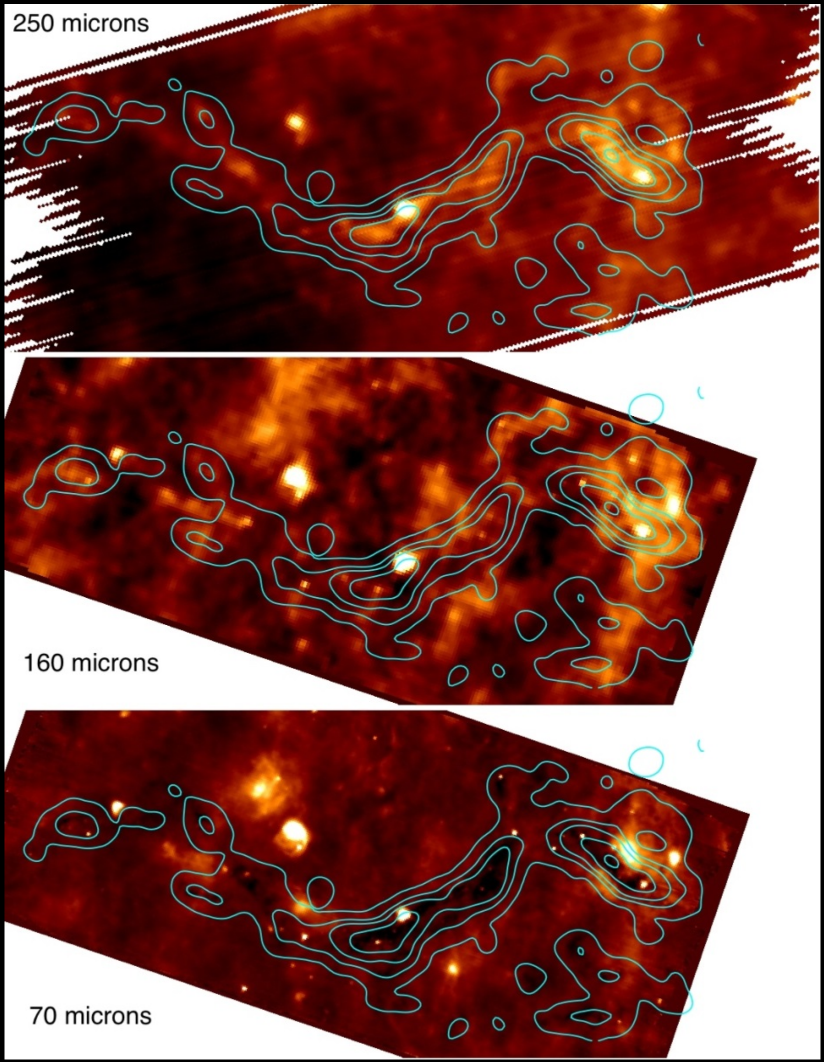

Colour continnuum; Contours NH_3

Henning et al. 2010

Limitations of Continuum Surveys

- Blending of emission along the line of sight
- Clumps are opaque in mid-IR
- Uncertain assumptions about dust parameters (κ, M_{dust}/M_{gas})
- No Distance Information
- No Kinematic Information

Spectral line surveys can overcome these shortcomings.

The Millimeter Astronomy Legacy Team 90 GHz (MALT 90) Survey

Science goal: How do high-mass star-forming molecular clumps evolve?

ATNF Mopra 22 m

MALT 90 provides

- **Distances**
- Column densities
- Virial masses
- Clump kinematics
- Molecular chemical abundances
- A large sample of the elusive youngest clumps

Why 90 GHz ?

- Molecular lines at ~90 GHz typically have high dipole moments, and therefore require high densities for their excitation (n > 10^5 cm^{-3})
- These lines are therefore sensitive ONLY to dense star-forming clumps.

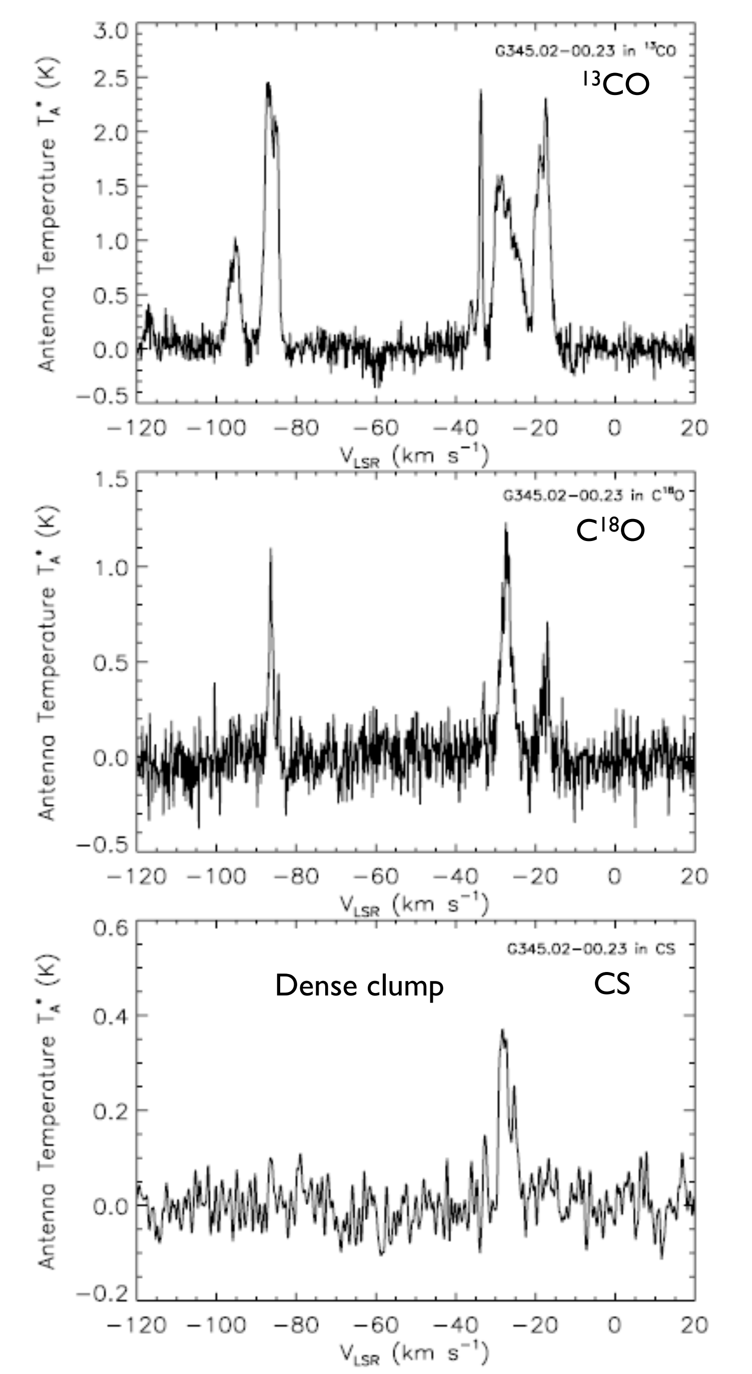

Deep MOPS integration G305

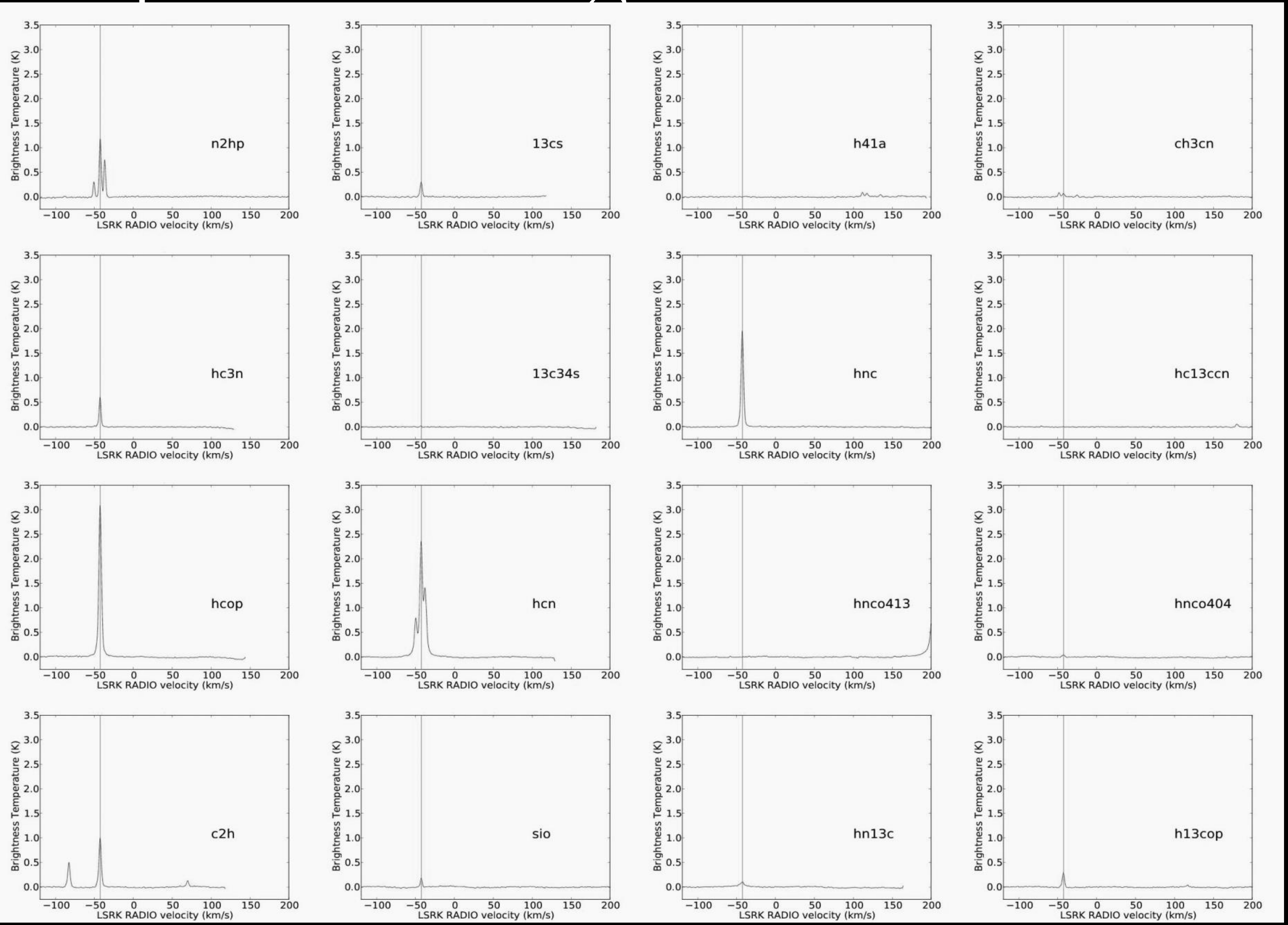

The MALT 90 Pilot Survey

- Test feasibility of large survey of dense clumps (Foster et al. 2011)
- Choose observing parameters
  - Source List
  - Map or single pointing
  - Spectral resolution

Foster et al. 2011

Strategy for a 90 GHz Survey

- A blind fully-sampled 90 GHz Galactic plane survey is impractical, because the 90 GHz line emission is relatively weak
- Must perform a TARGETED survey based on dense cores discovered by other surveys
- We choose the ATLASGAL 870 μm dust continuum survey
  - Sensitive to high column density clumps
  - Sensitive to both cold and warm clumps

Useful Surveys

- HOPS: NH_3 (1,1) and (2,2)
- ATLASGAL: 870 μm dust continuum
- IRAS: far-infrared continuum
- MIPSGAL: 24 μm
- GLIMPSE: 3 to 8 μm (dark and bright)

Pilot Survey: Choose ATLASGAL 870 μm as preferred source list

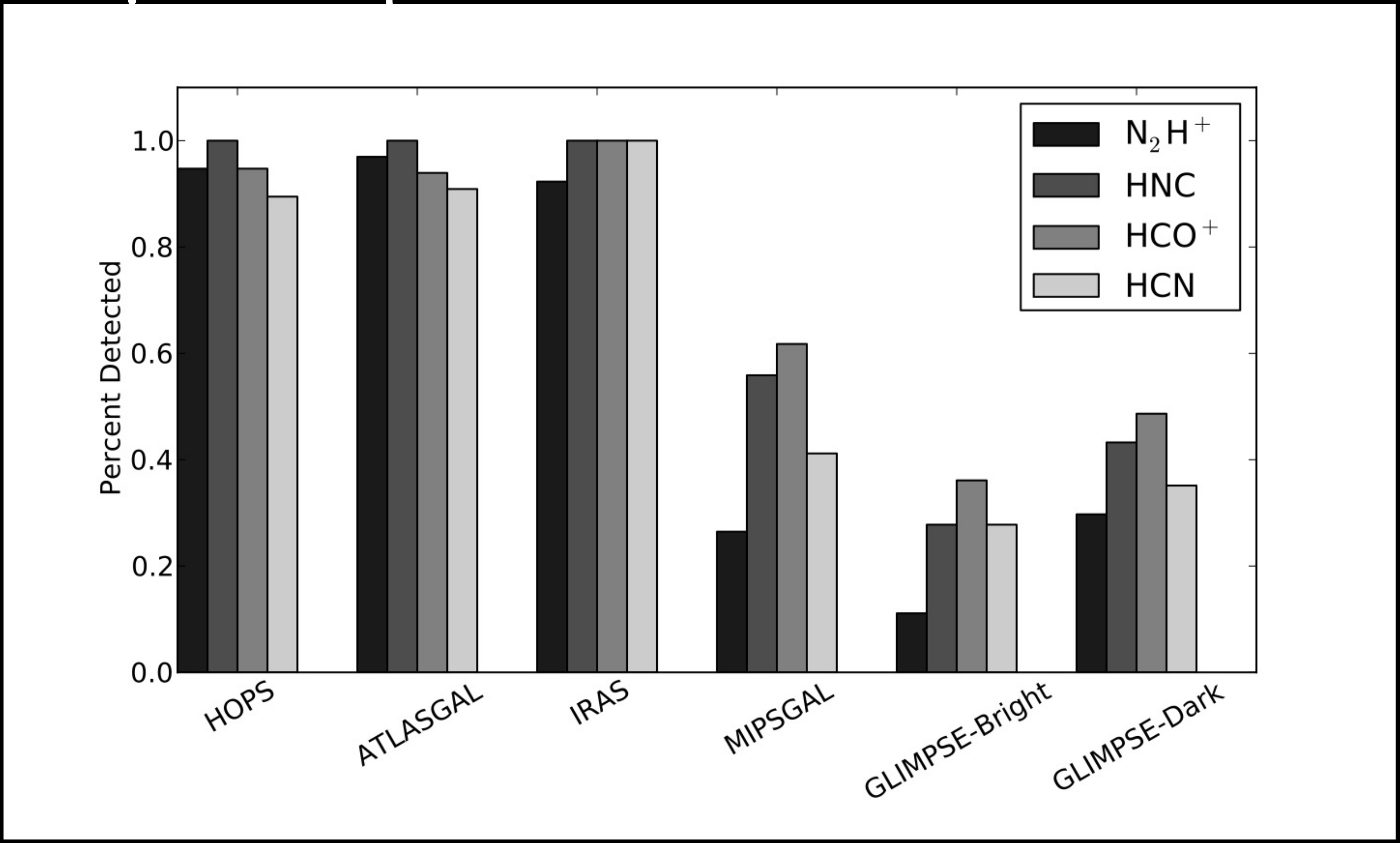

Foster et al. 2011

Differing complex chemical morphologies:

N_2H^+

need to map

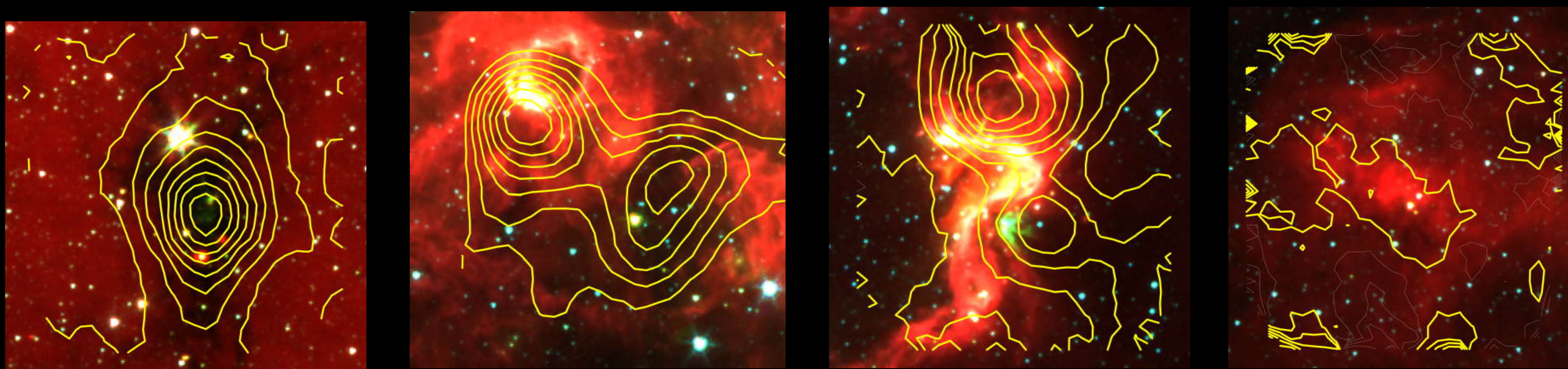

HCO^+

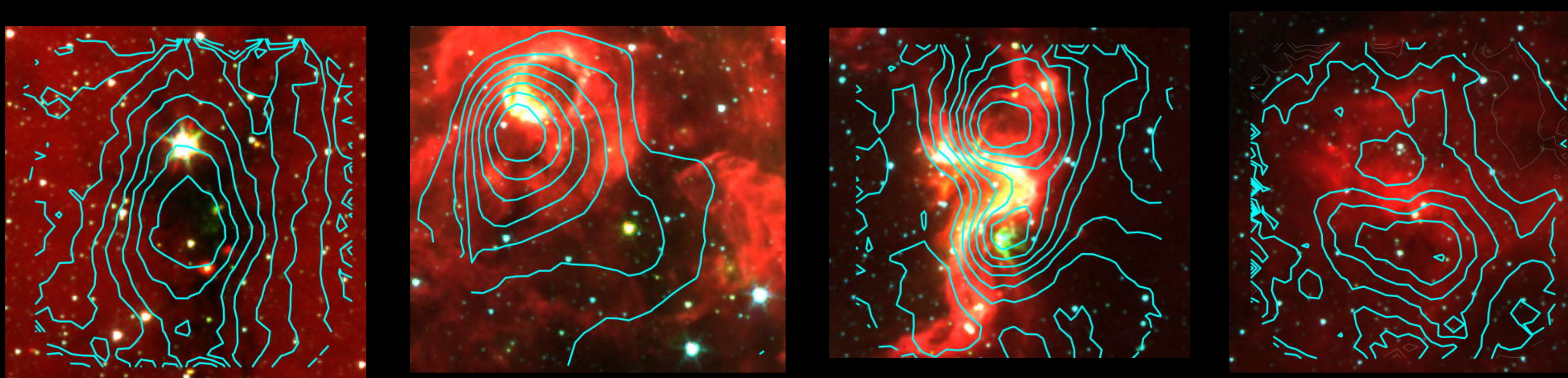

GLIMPSE 3-colour image

Foster et al. 2011

Complex Line Profiles: Need sufficient spectral resolution

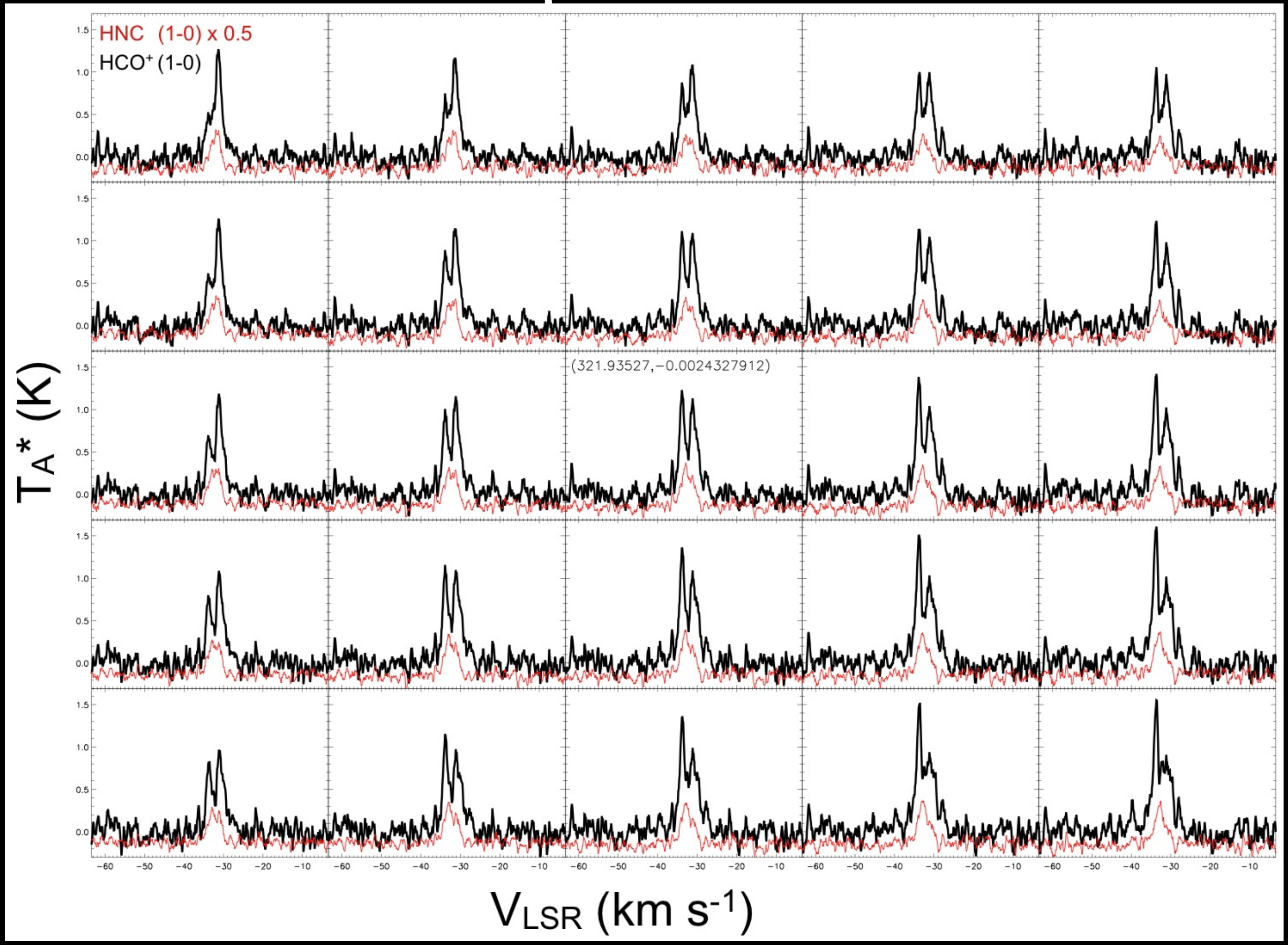

Complex Line Profiles: Need good spectral resolution

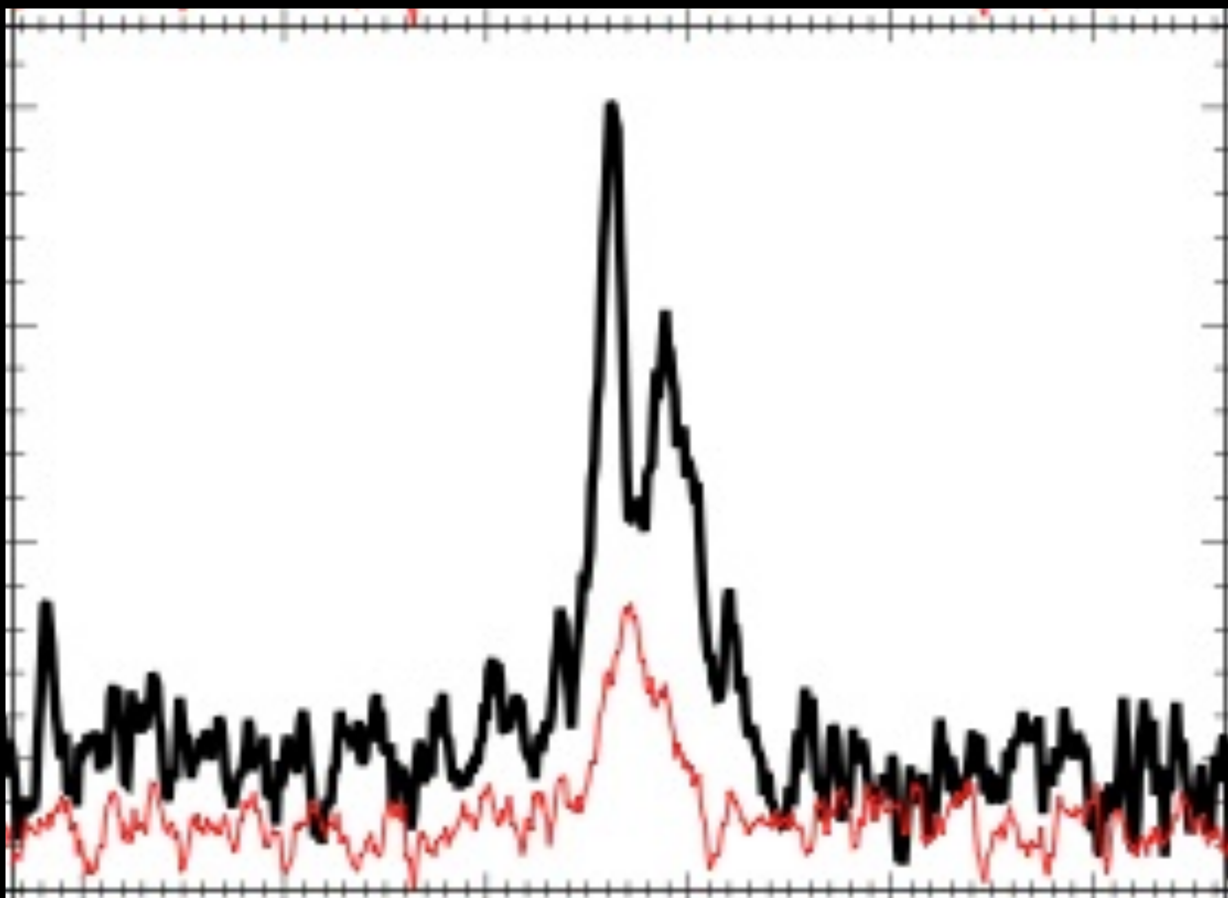

---- HCO^+ thick
---- $H^{13}CO^+$ thin

Foster et al. 2011

Hot vs. Cold Core 90 GHz spectra

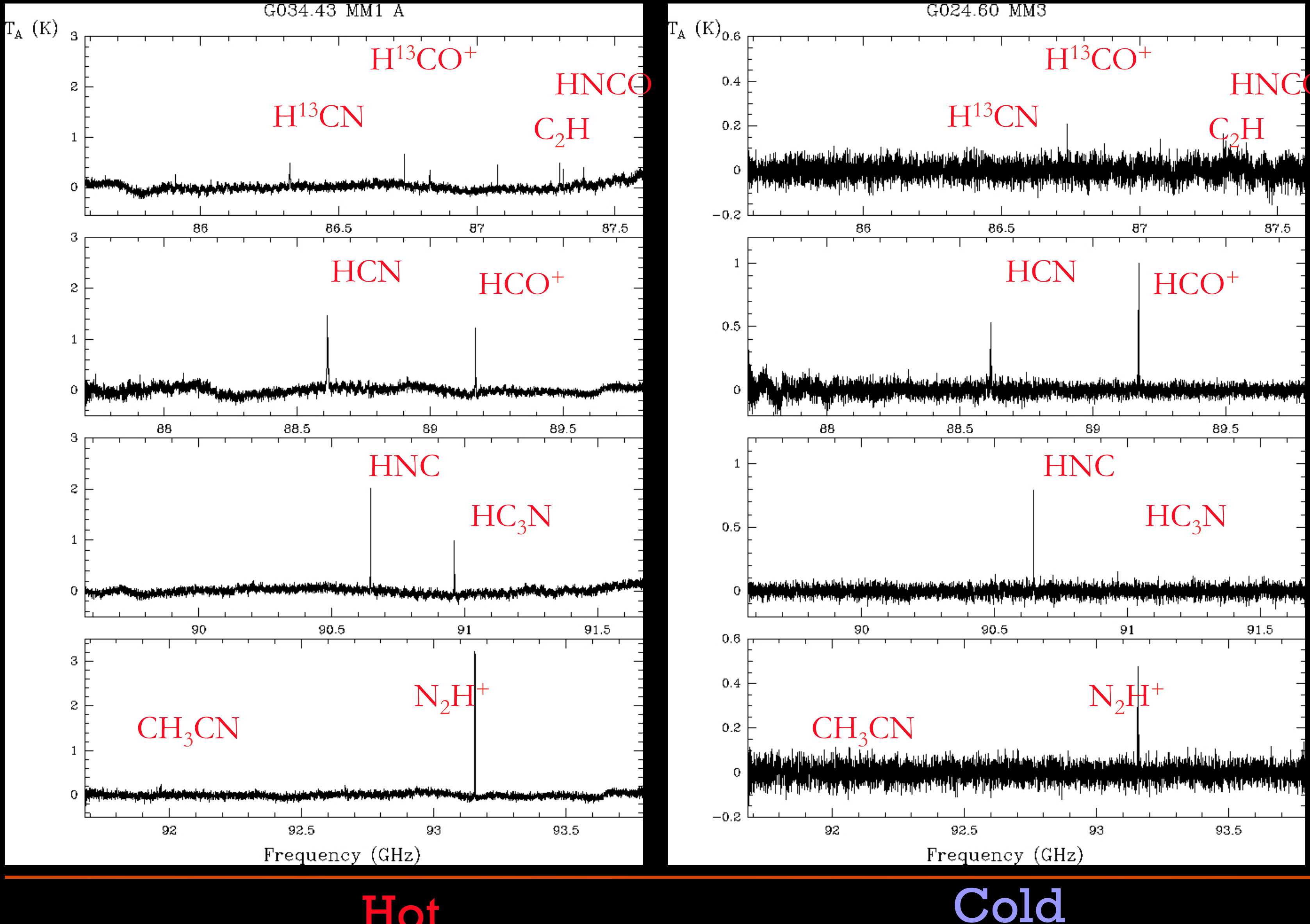

MALT 90: Scope of the project

- MALT 90 imaged 2,014 high-mass cores with Mopra in **16** key 90 GHz molecular lines, e.g. N_2H^+, HCO^+, HCN, HNC…
- The survey is **complete**: all high-mass star forming clumps (M > 200 $M_\odot$) to 10 kpc.
- It provides complementary information to the continuum surveys, especially distances.
- MALT 90 sources will be key targets for ALMA

ALMA can image any core detected in MALT 90 at 1" angular resolution with excellent signal-to-noise

All of these cores are strong molecular line emitters easily detected by Mopra

0.2 degrees

1.2 degrees

For more on Nessie see Jackson et al. 2010 ApJL

Mopra HNC (1-0) integrated emission

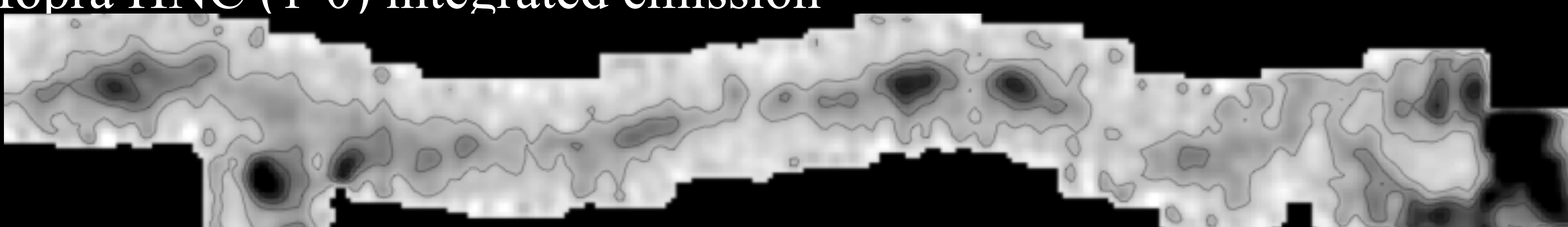

Blue - 3.6μm, Green - 8μm, Red - 24μm

Image credit: NASA/JPL-Caltech/Univ. of Wisconsin

MALT 90 Survey Observing Parameters

Targets: ATLASGAL 870 μm clumps

16 lines near 90 GHz

3’ x 3’ maps

38” angular resolution

0.05 K sensitivity

0.1 km s^{-1} spectral resolution

$-60^{o} >$ long. $> +20^{o}$

(Jackson et al. 2013)

ATNF Mopra 22 m

Jackson et al. 2013

16 Selected Lines

IF	Line	Frequency (MHz)	Tracer
1	N_2H^+	93,173.772	Density, chemically robust
2	^{13}CS	92,494.303	Optical depth, Column density, V_{LSR}
3	H41α	92,034.475	Ionized gas
4	CH_3CN	91,985.316	Hot core
5	HC_3N	91,199.796	Hot core
6	$^{13}C^{34}S$	90,926.036	Optical depth, Column density, V_{LSR}
7	HNC	90,663.572	Density; cold chemistry
8	$HC^{13}CCN$	90,593.059	Hot core
9	HCO+	89,188.526	Density
10	HCN	88,631.847	Density
11	HNCO 4_{13}	88,239.027	Hot core
12	HNCO 4_{04}	87,925.238	Hot core
13	C_2H	87,316.925	Photodissociation region
14	SiO	86,847.010	Shock/outflow
15	$H^{13}CO^+$	86,754.330	Optical depth, Column density, V_{LSR}
16	$H^{13}CN$	86,340.167	Optical depth, Column density, V_{LSR}

MALT 90 is completed

- 2,014 maps
- 3,566 clumps

All data are now released:

http://atoa.atnf.csiro.au/MALT90

Catalog paper (Rathborne et al.) will be submitted within a month

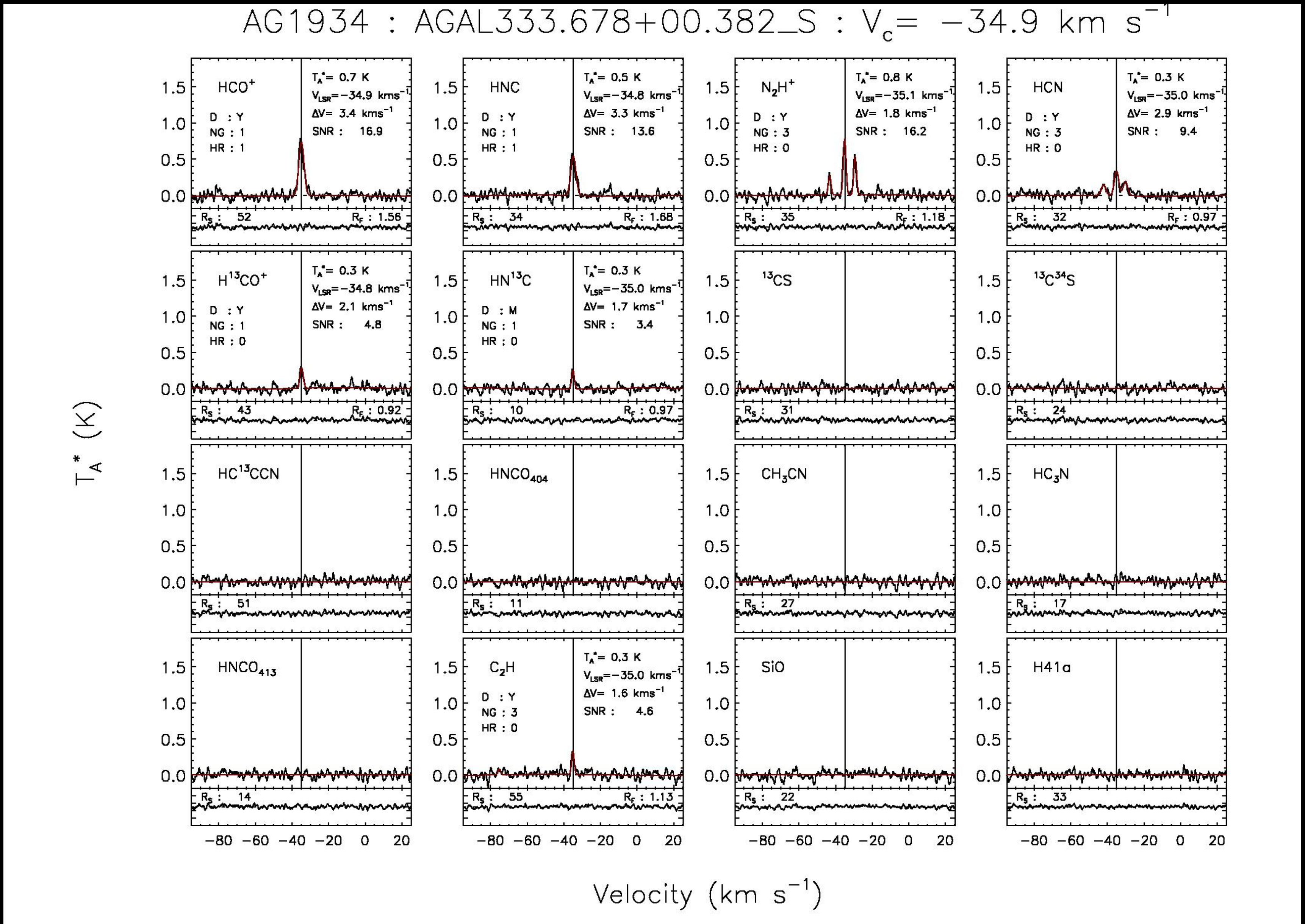
AG1934 : AGAL333.678+00.382_S : Vc= −34.9 km s−1
HCO+
TA*= 0.7 K
VLSR=−34.9 kms−1
ΔV= 3.4 kms−1
SNR : 16.9
D : Y
NG : 1
HR : 1
RS : 52
RF : 1.56
HNC
TA*= 0.5 K
VLSR=−34.8 kms−1
ΔV= 3.3 kms−1
SNR : 13.6
D : Y
NG : 1
HR : 1
RS : 34
RF : 1.68
N2H+
TA*= 0.8 K
VLSR=−35.1 kms−1
ΔV= 1.8 kms−1
SNR : 16.2
D : Y
NG : 3
HR : 0
RS : 35
RF : 1.18
HCN
TA*= 0.3 K
VLSR=−35.0 kms−1
ΔV= 2.9 kms−1
SNR : 9.4
D : Y
NG : 3
HR : 0
RS : 32
RF : 0.97
H13CO+
TA*= 0.3 K
VLSR=−34.8 kms−1
ΔV= 2.1 kms−1
SNR : 4.8
D : Y
NG : 1
HR : 0
RS : 43
RF : 0.92
HN13C
TA*= 0.3 K
VLSR=−35.0 kms−1
ΔV= 1.7 kms−1
SNR : 3.4
D : M
NG : 1
HR : 0
RS : 10
RF : 0.97
13CS
RS : 31
13C34S
RS : 24
HC13CCN
RS : 51
HNCO404
RS : 11
CH3CN
RS : 27
HC3N
RS : 17
HNCO413
RS : 14
C2H
TA*= 0.3 K
VLSR=−35.0 kms−1
ΔV= 1.6 kms−1
SNR : 4.6
D : Y
NG : 3
HR : 0
RS : 55
RF : 1.13
SiO
RS : 22
H41α
RS : 33
TA* (K)
Velocity (km s−1)

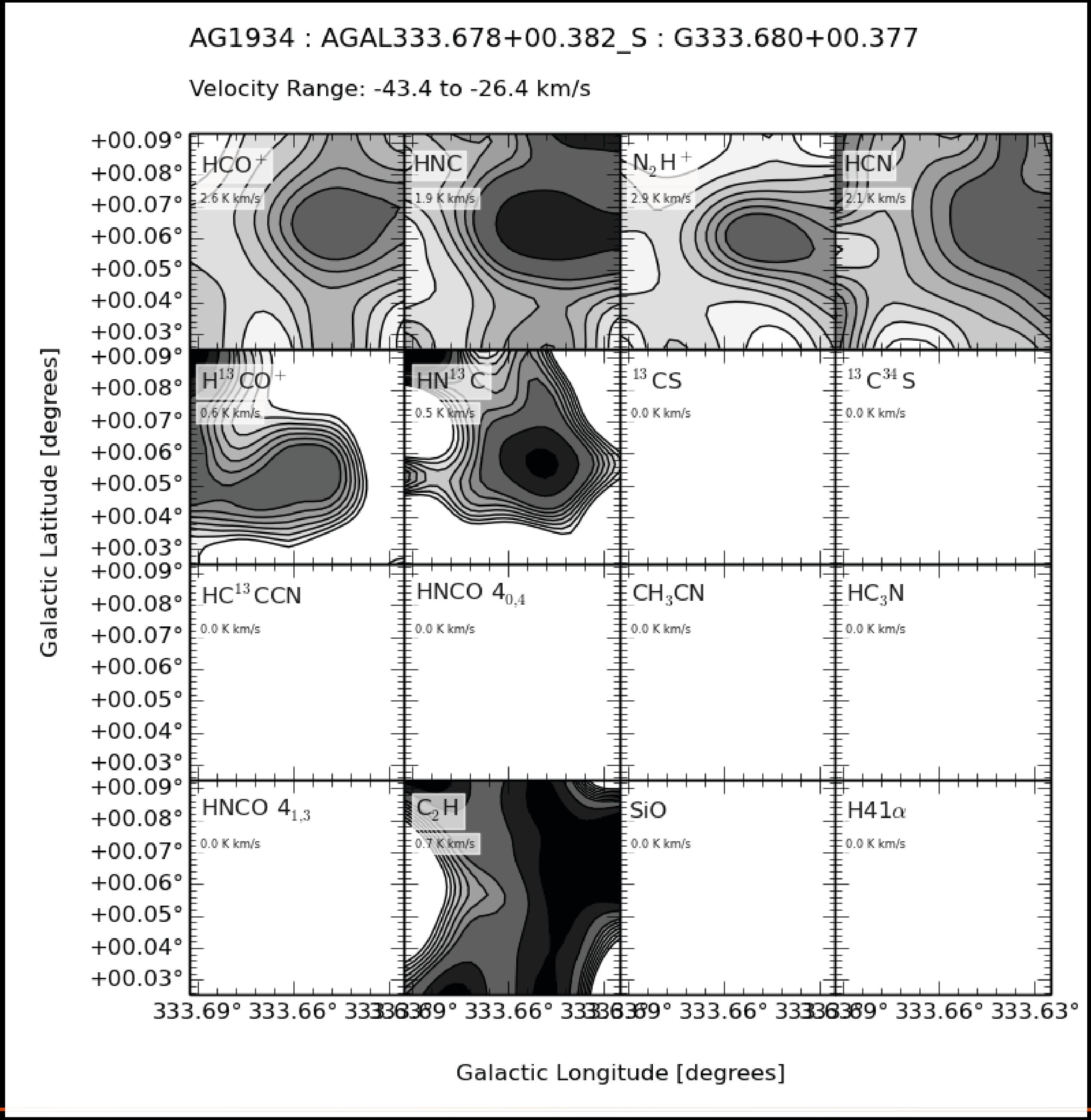

AG1934 : AGAL333.678+00.382_S : G333.680+00.377
Velocity Range: -43.4 to -26.4 km/s
HCO+
2.6 K km/s
HNC
1.9 K km/s
N2H+
2.9 K km/s
HCN
2.1 K km/s
H13CO+
0.6 K km/s
HN13C
0.5 K km/s
13CS
0.0 K km/s
13C34S
0.0 K km/s
HC13CCN
0.0 K km/s
HNCO 40,4
0.0 K km/s
CH3CN
0.0 K km/s
HC3N
0.0 K km/s
HNCO 41,3
0.0 K km/s
C2H
0.7 K km/s
SiO
0.0 K km/s
H41α
0.0 K km/s
Galactic Latitude [degrees]
+00.09° +00.08° +00.07° +00.06° +00.05° +00.04° +00.03°
333.69° 333.66° 333.63°
Galactic Longitude [degrees]

Some MALT 90 highlights

- Distances
- Evolution
  - Collapse motions
  - Maser activity
- The Gao-Solomon HCN-FIR relation for clumps: ties to extragalactic astronomy

Yanett Contreras will discuss more results in the next talk.

1. Kinematic Distances

- We can measure the distances kinematically
- If the Galaxy's "rotation curve" $V_{circ}(r)$ is known, then a distance can be deduced from the measured velocity.

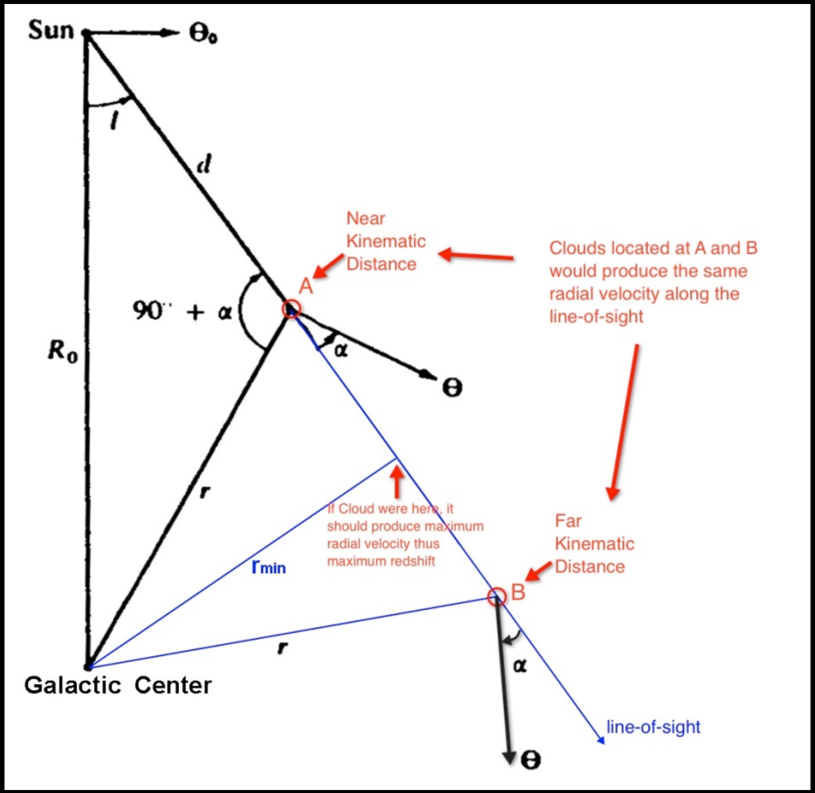

$$= R_0 \sin l \, V(r)/v_r + v_0 \sin l \qquad d = R_0 \cos l \pm \sqrt{r^2 - R_0^2 (\sin l)^2}$$

Whitaker et al. 2013

1. Kinematic Distances

- We can measure the distances kinematically
- If the Galaxy's "rotation curve" $V_{circ}(r)$ is known, then a distance can be deduced from the measured velocity.

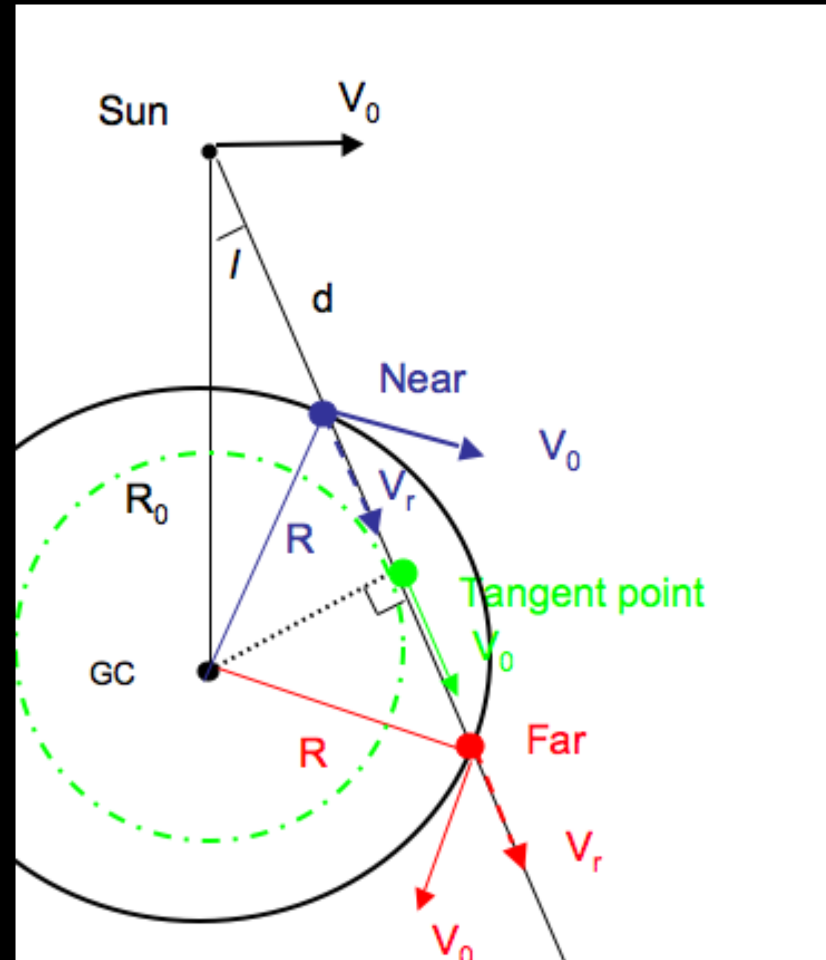

$$= \frac{R_0 \sin l \, V(r)}{v_r + v_0 \sin l} \qquad d = R_0 \cos l \pm \sqrt{r^2 - R_0^2 (\sin l)^2}$$

Whitaker et al. 2013

Continuum Absorption

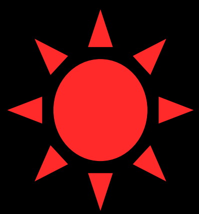

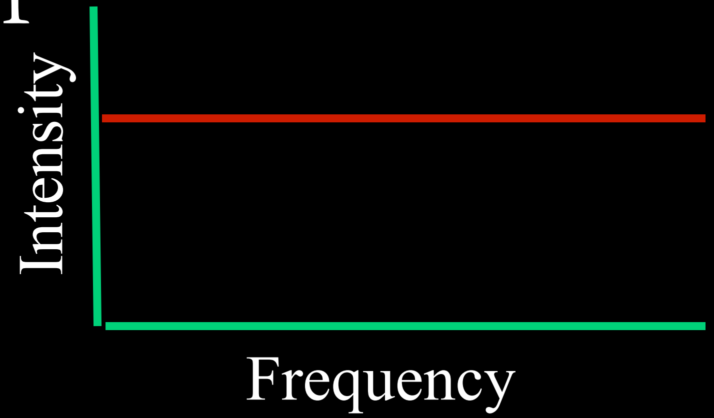

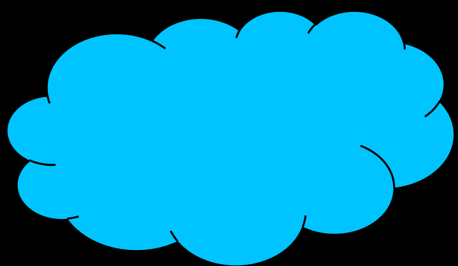

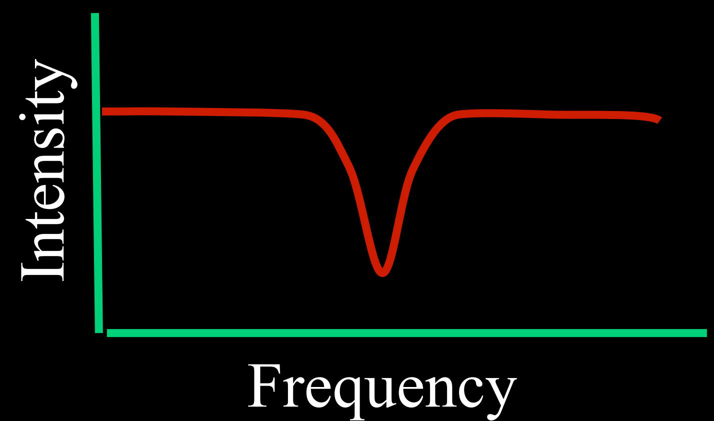

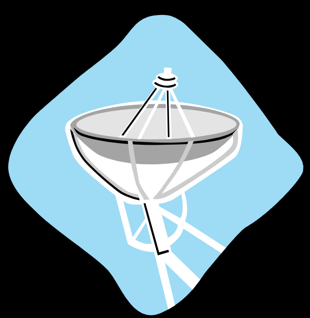

Line (Self-)Absorption

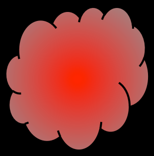

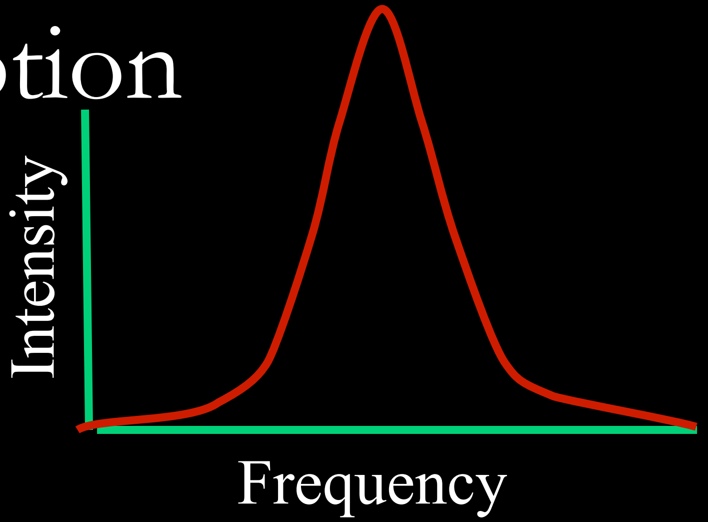

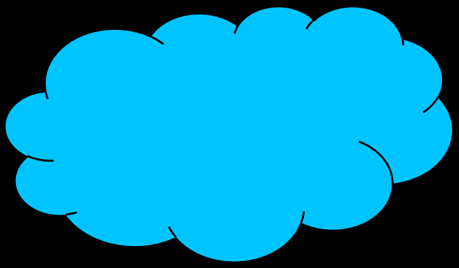

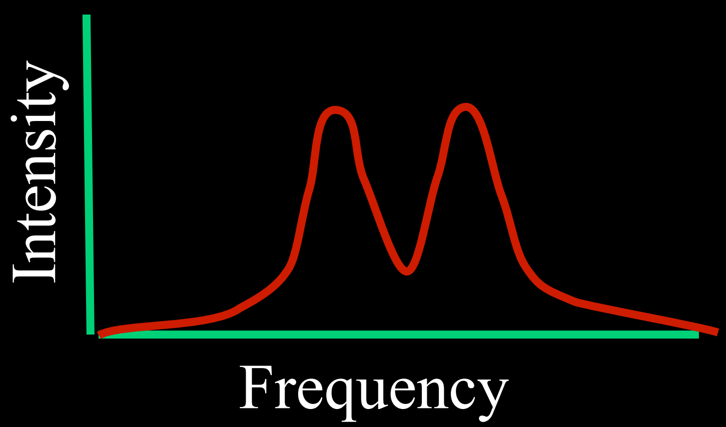

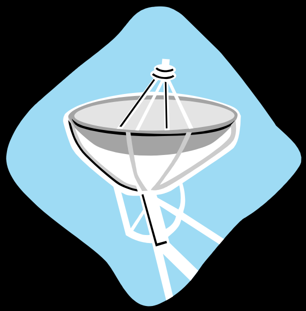

Resolving the Near/Far Kinematic Distance Ambiguity with H I 21 cm

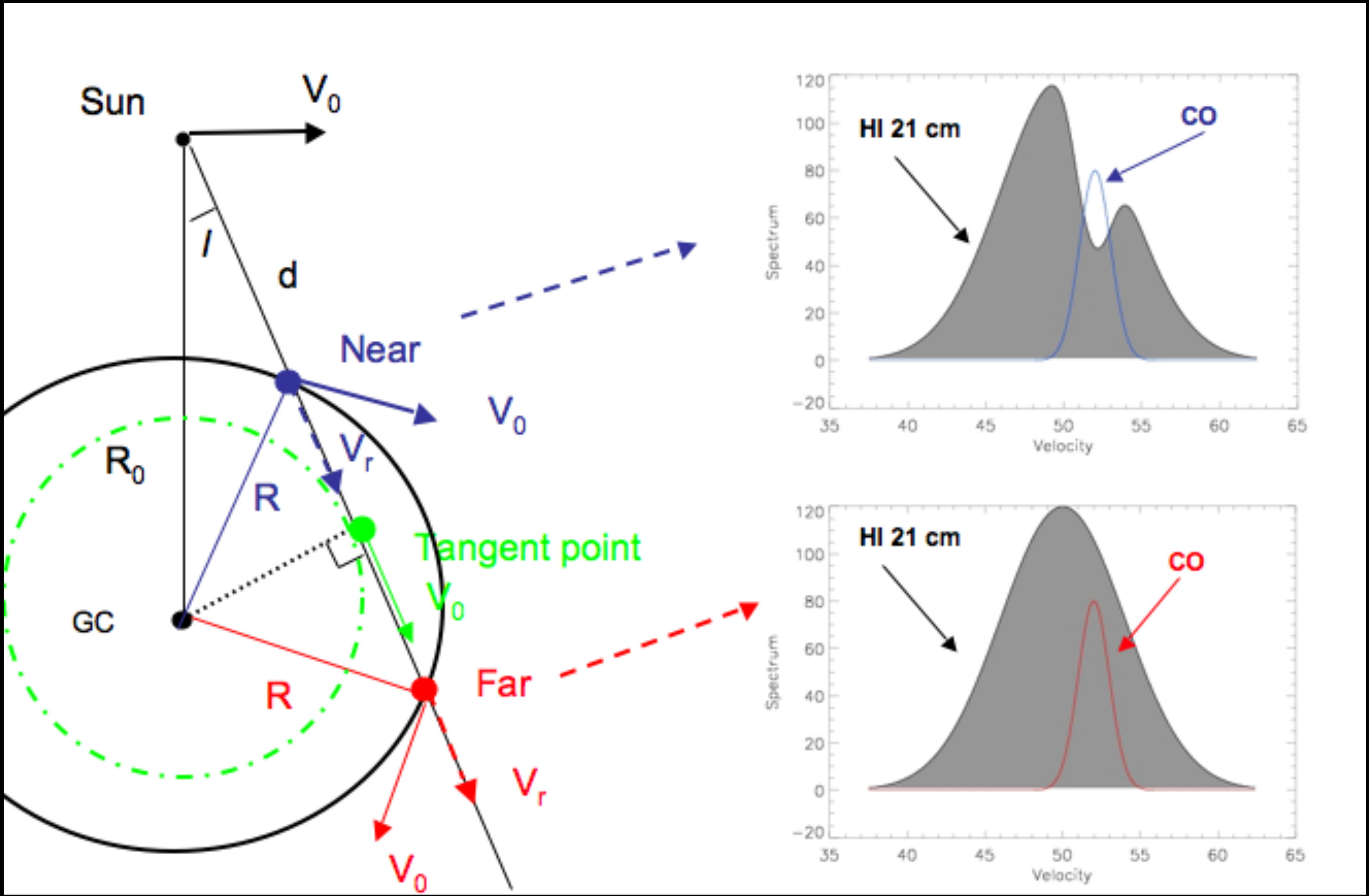

Resolving the Near/Far Kinematic Distance Ambiguity with H I 21 cm

Near Far

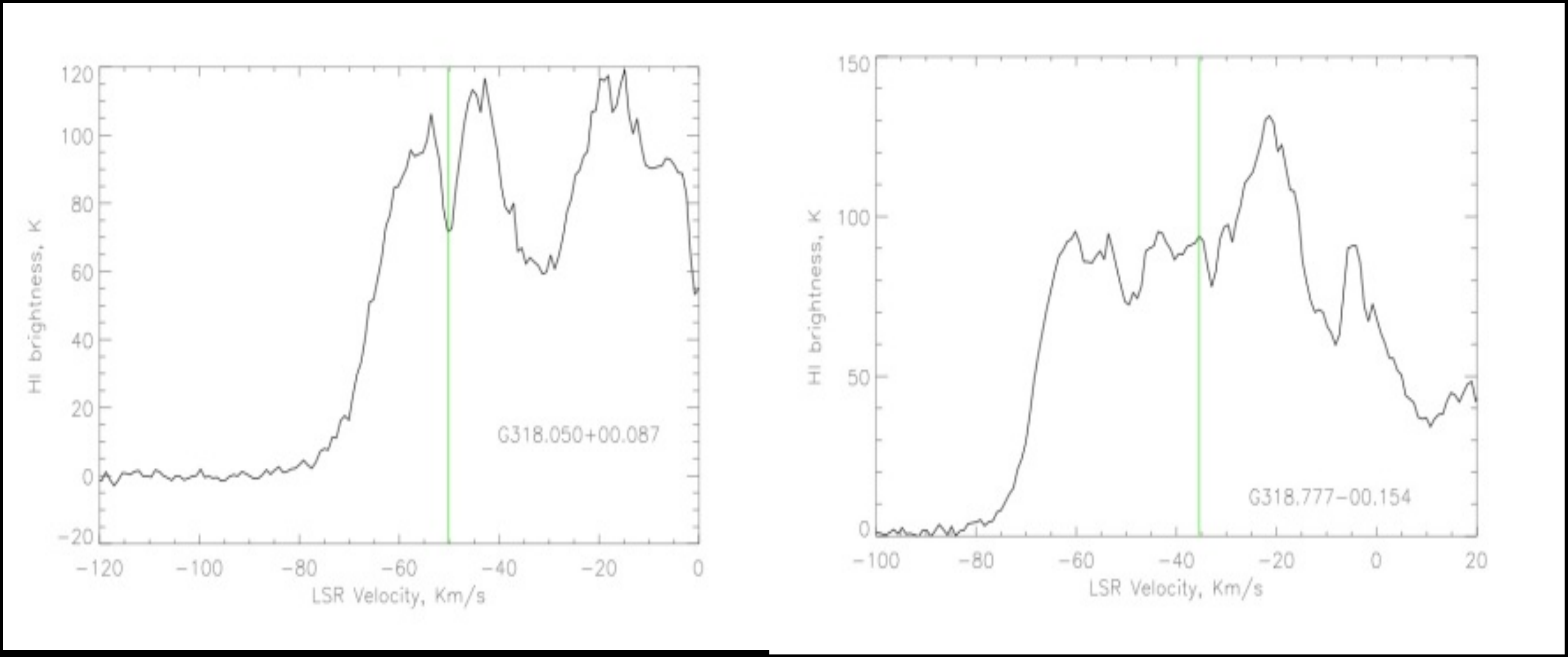

Clump velocity from MALT90

Kinematic Distances: Longitude and velocity of MALT 90 clumps

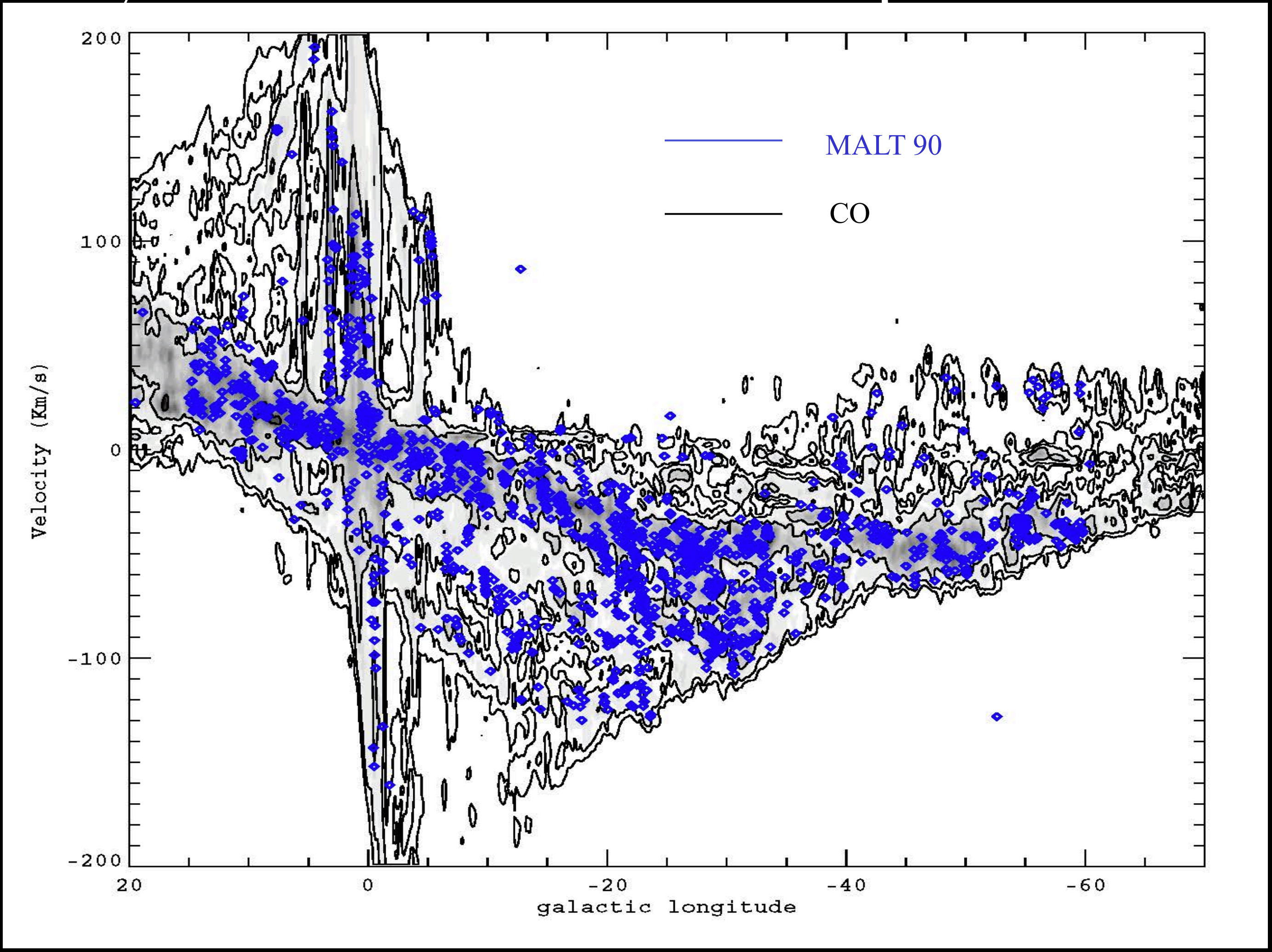

Source: CfA-Columbia CO survey   Dame et al. 2001

Whitaker et al. 2014

Galactic Distribution of Clumps

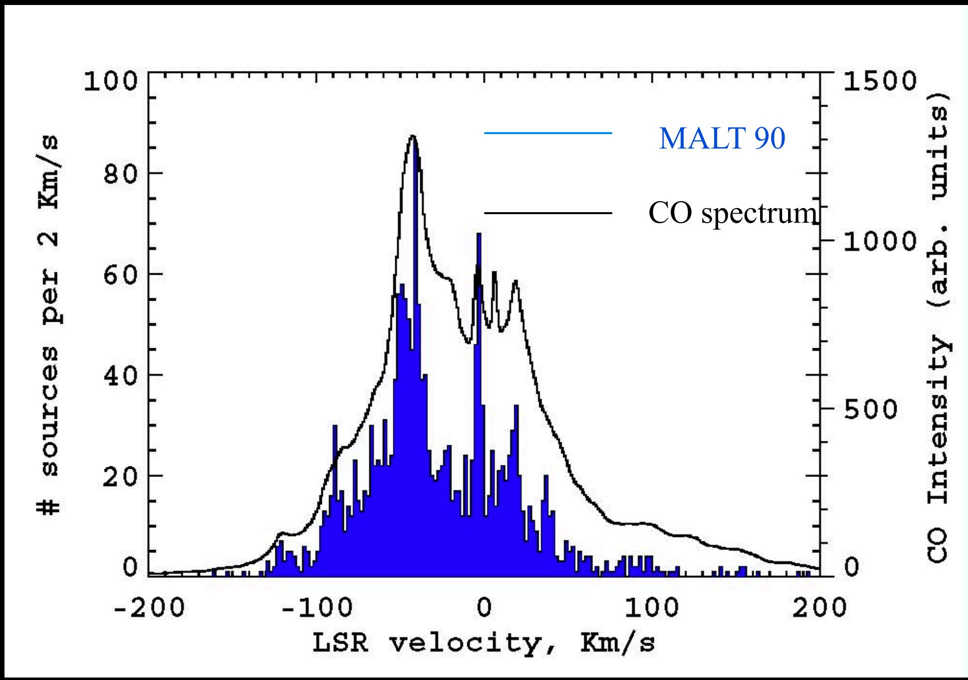

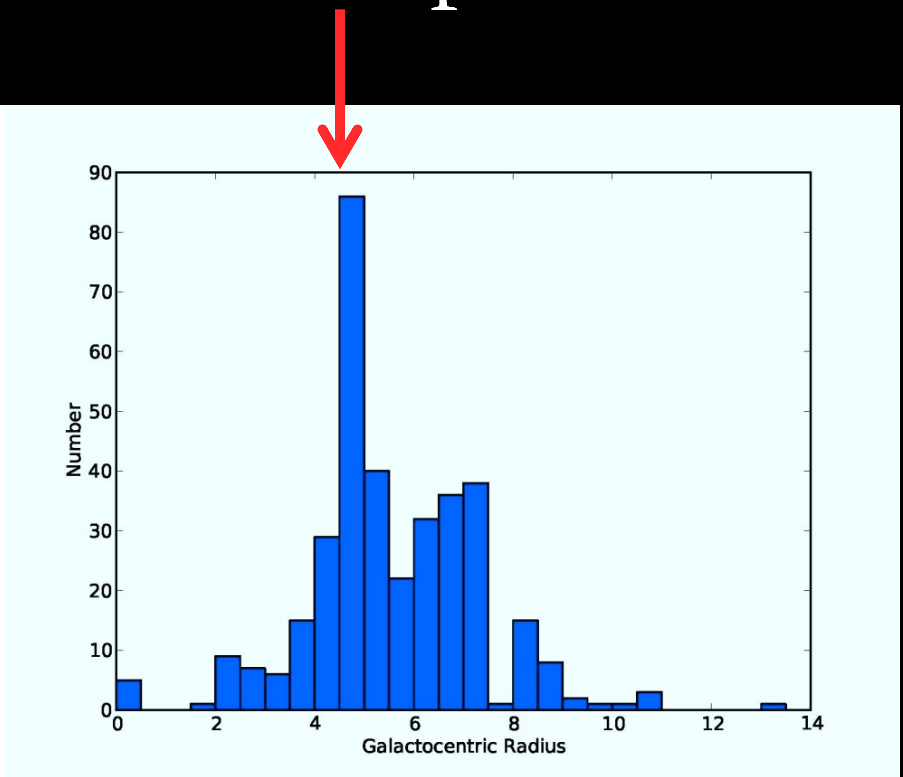

Spiral Arm

Source: CfA-Columbia CO survey Dame et al. 2001

Whitaker et al. 2014

Galactic Distribution

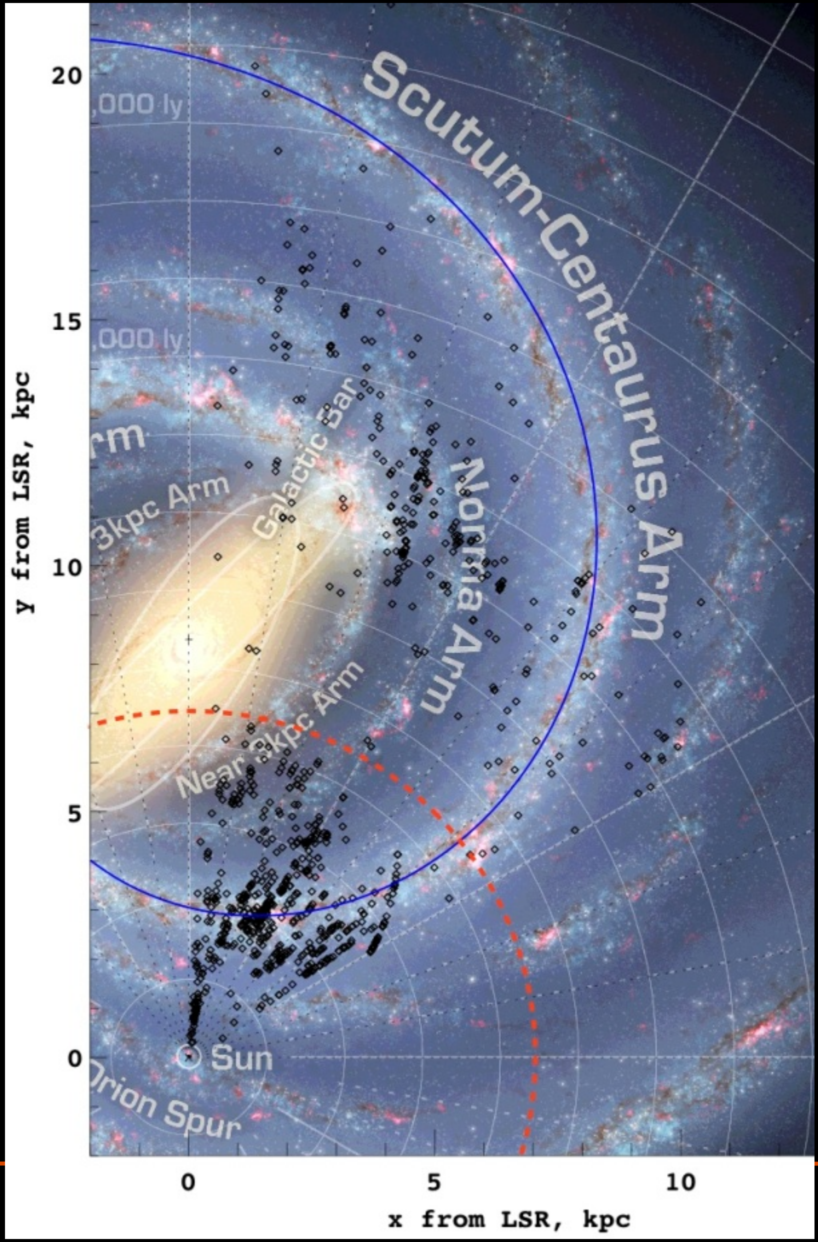

The cores are associated with spiral arms, including the heretofore unseen "far" portions of Norma and Scutum-Centaurus.

Galactic Distribution: MALT 90

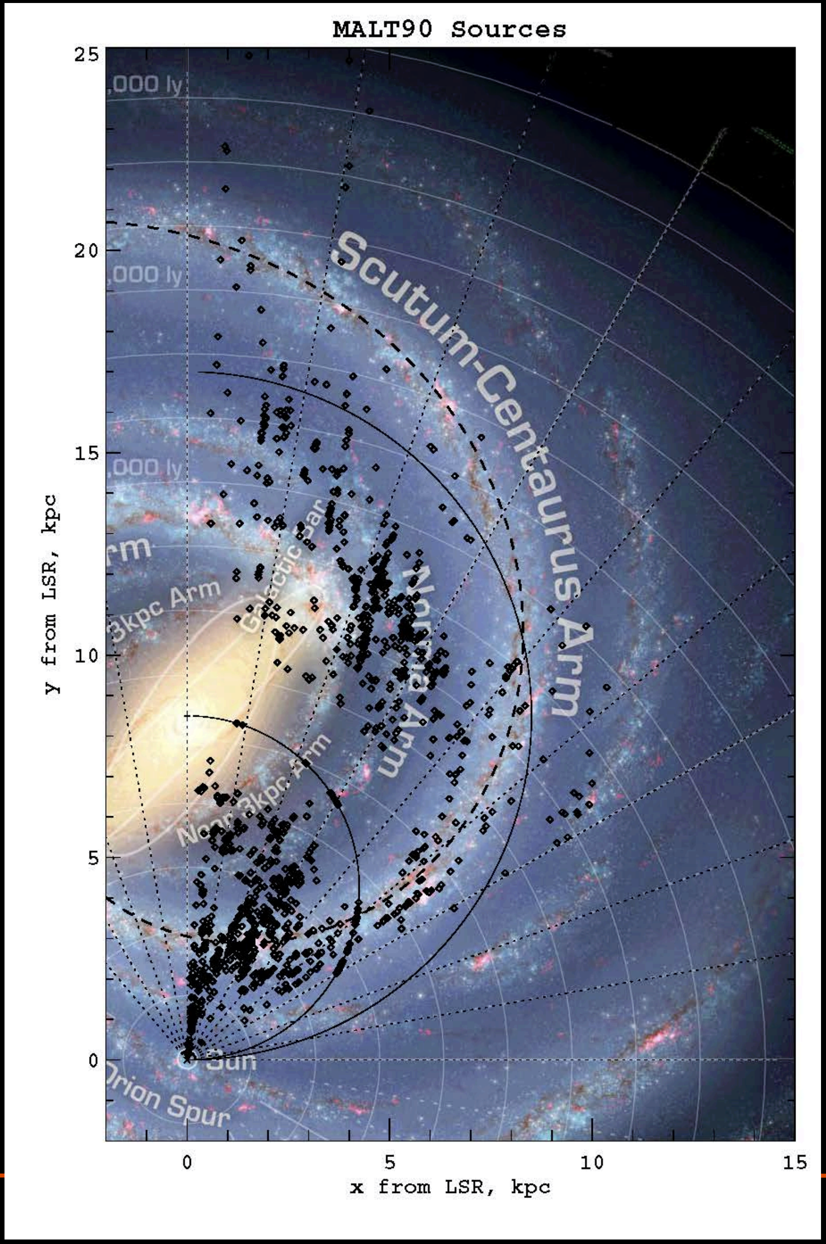

The clumps are associated with spiral arms, possibly including the heretofore unseen "far" portions of Norma and Scutum-Centaurus.

Whitaker et al. in prep

2. Evolution: Temperature and Column Density

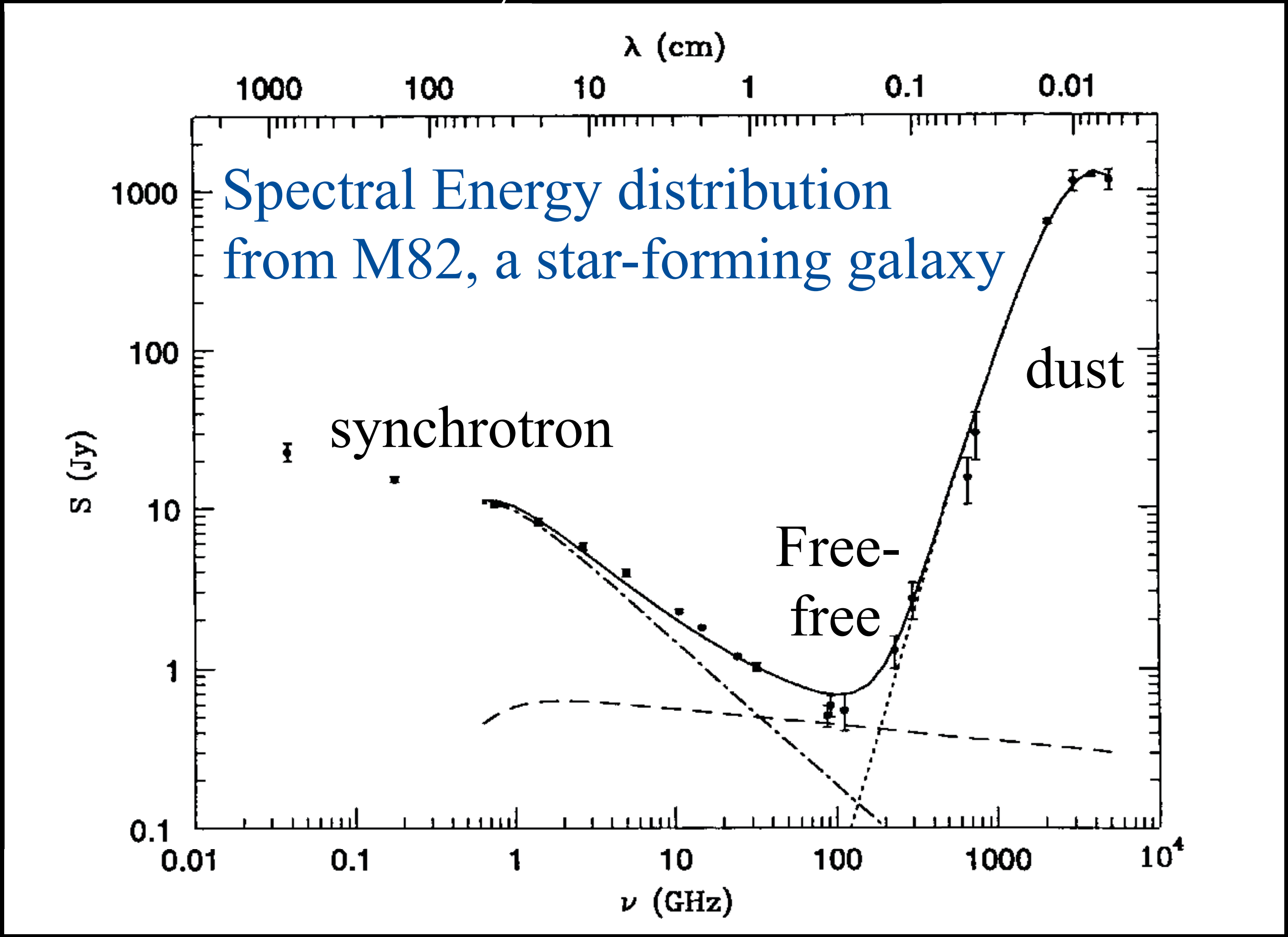

Use Herschel data in the far-infrared and submillimetre to find T_{dust} and N

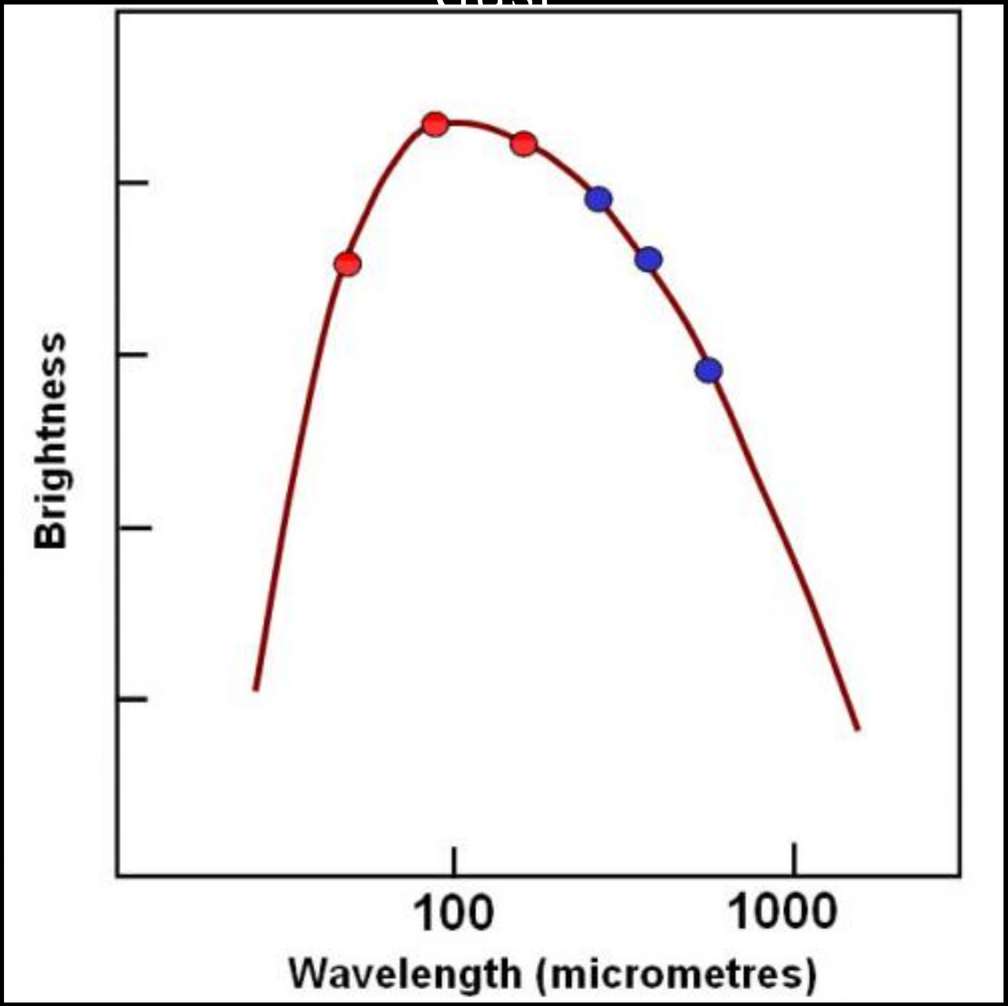

Temperature and Column Density Evolution

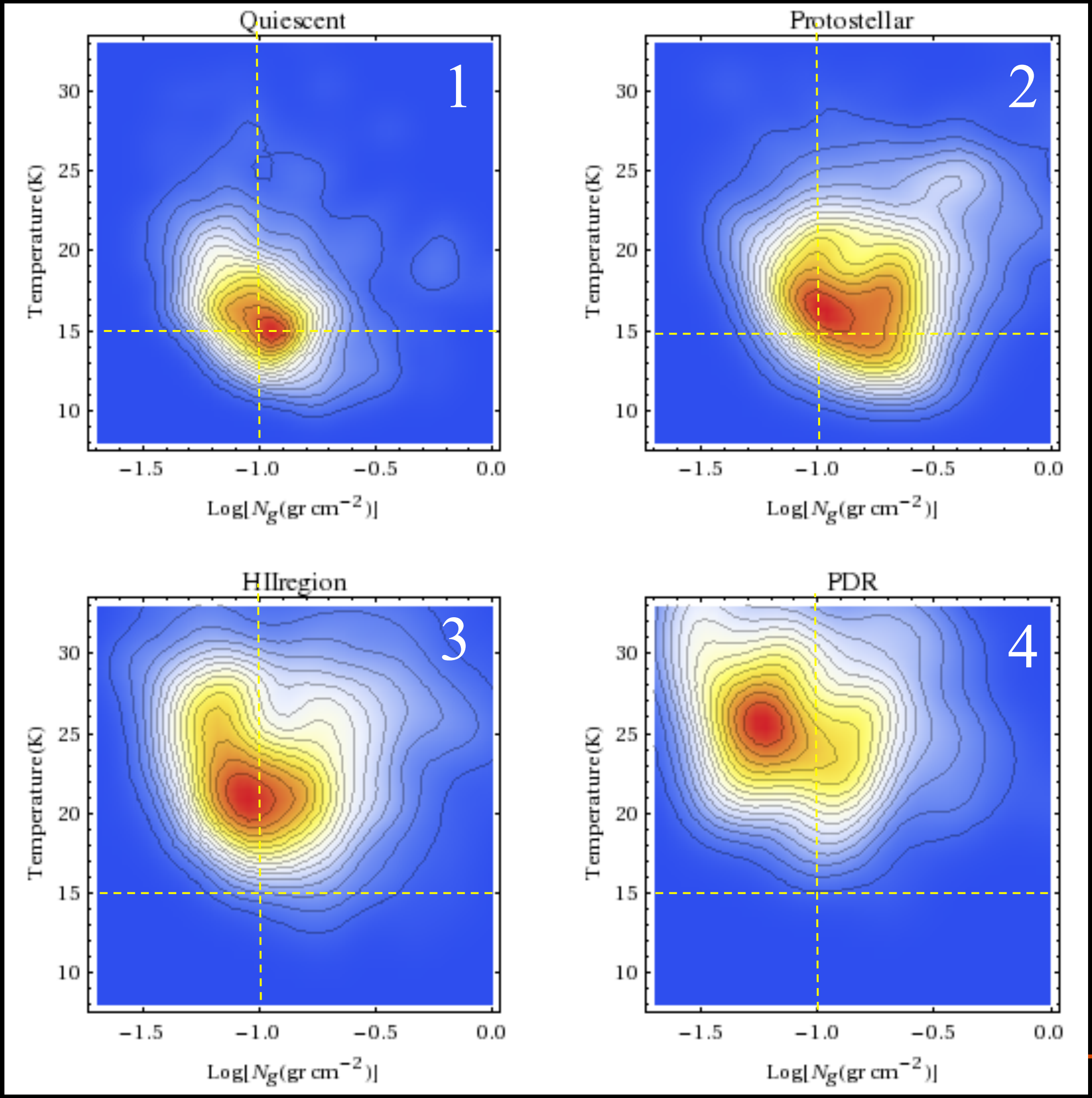

The Herschel data indicate evolution.

The clumps' dust temperature increases from 15 to 25 K. Column densities increase, then decrease

Guzman et al. 2014

Evolution of luminosity

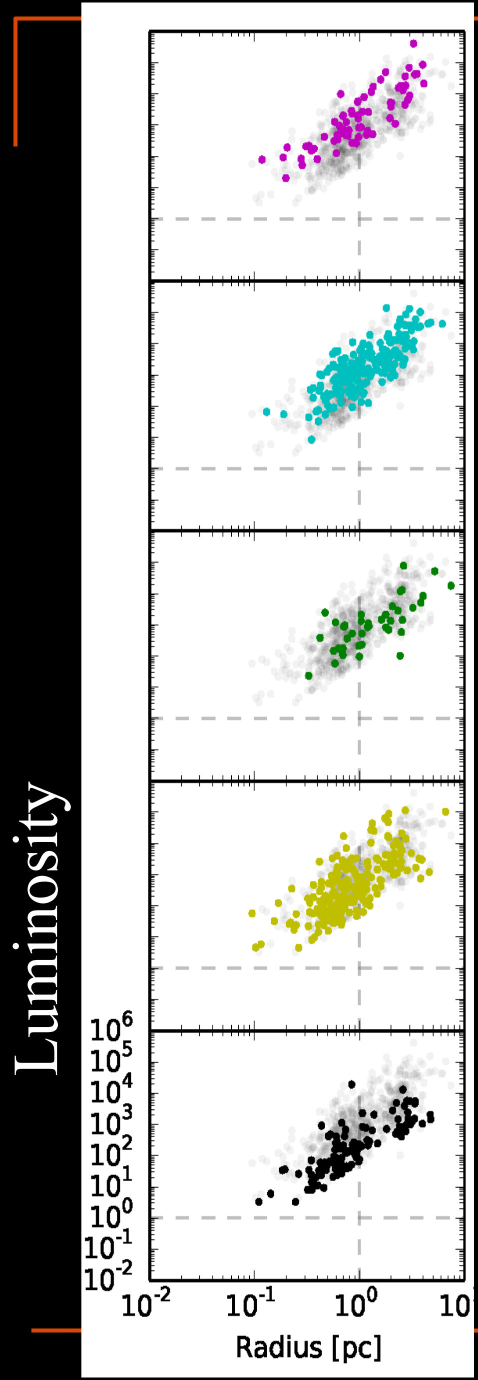

- The luminosity of clumps evolves
- Later stages are more luminous

Chemical Evolution: HNC/HCN

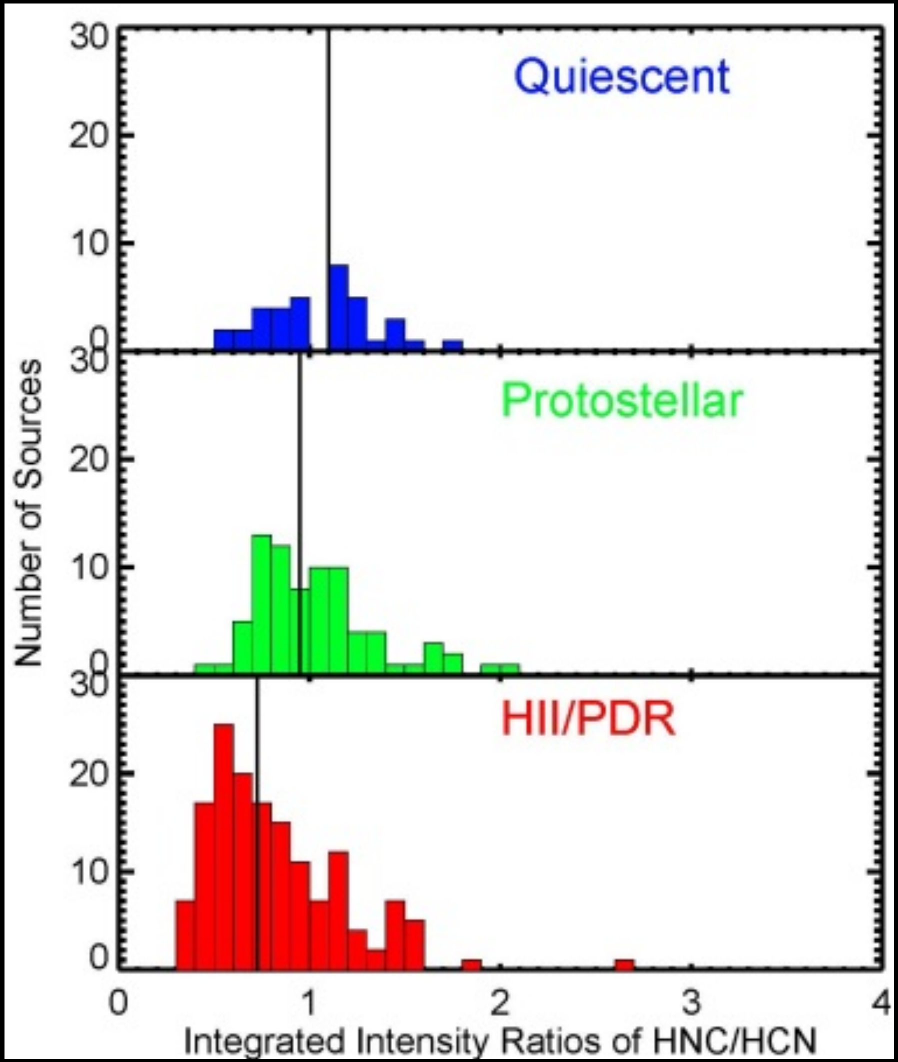

HNC favored in cold cores due to chemical fractionation (same parent molecule $HNCH^+$)

The chemistry of cores evolves with time.

Hoq et al. 2013

2. Evolution: Chemistry

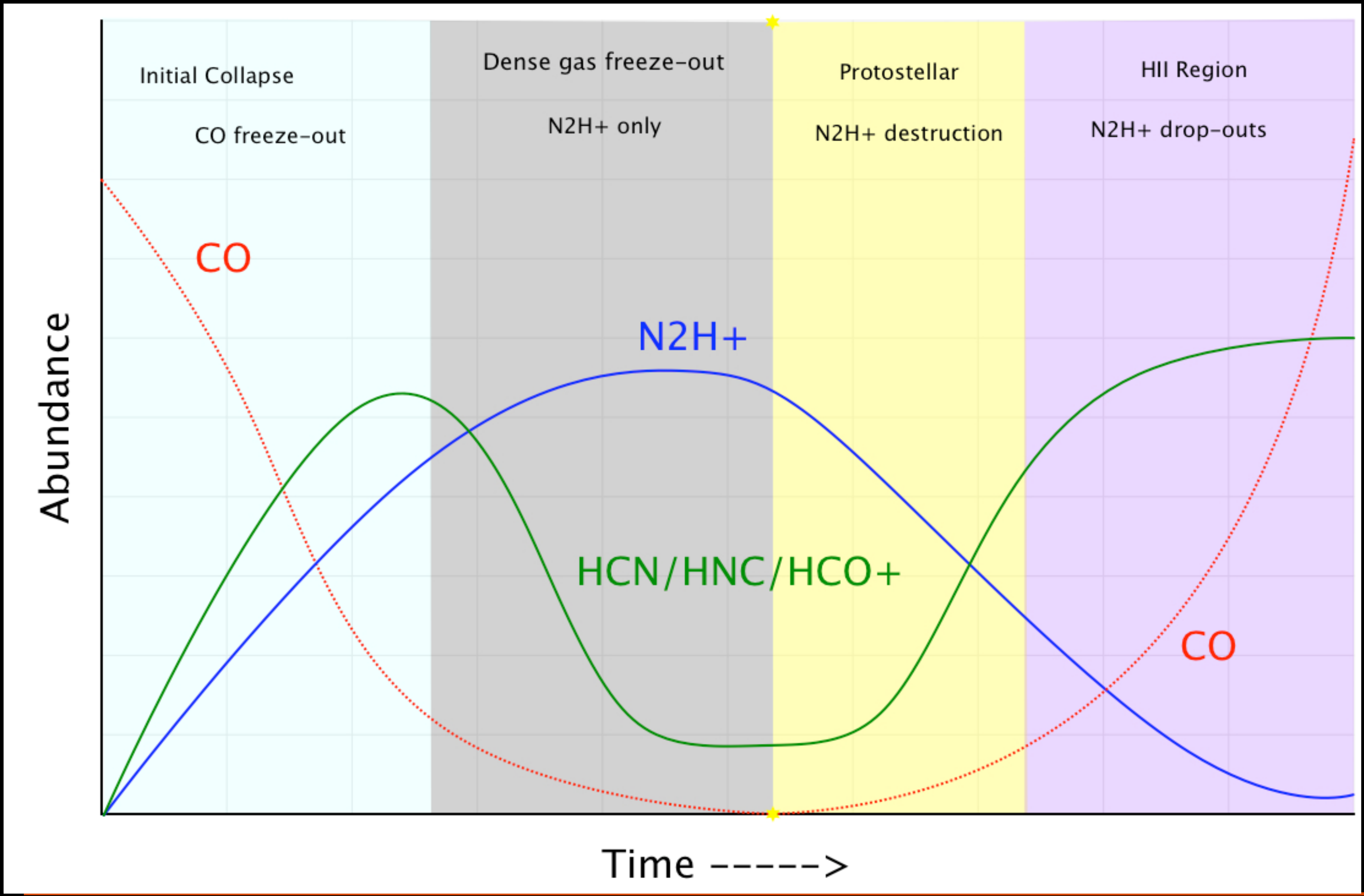

Based on chemical models of Lee et al. (2004); see also Bergin (2007)

An N_2H^+ "rich" source $I(N_2H^+) > 3*I(HCO^+)$

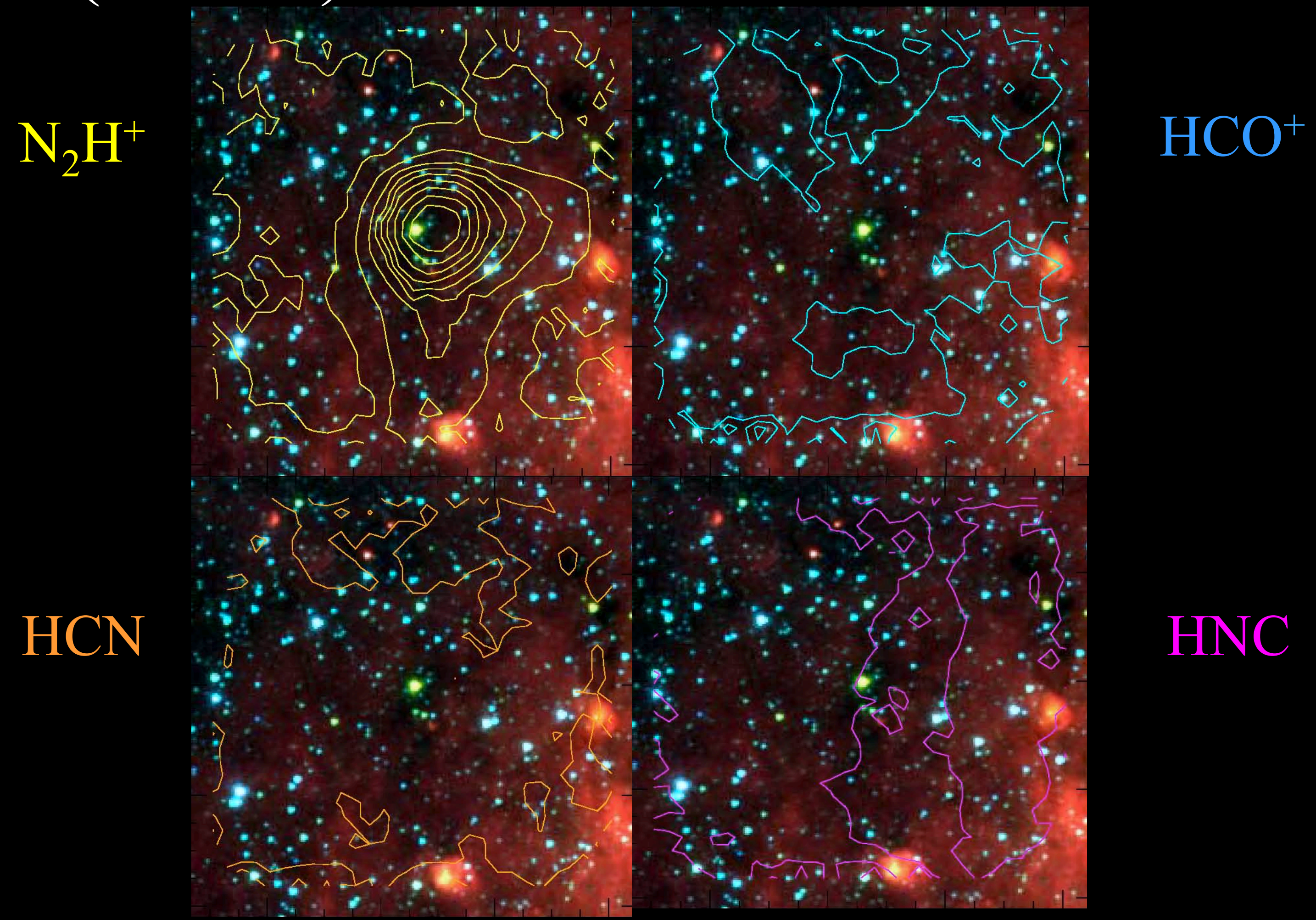

Blue - 3.6μm, Green - 4.5μm, Red – 8 μm from GLIMPSE survey

Hoq et al. 2013

An N_2H^+ "poor" source

$I(N_2H^+) < 3*I(HCO^+)$

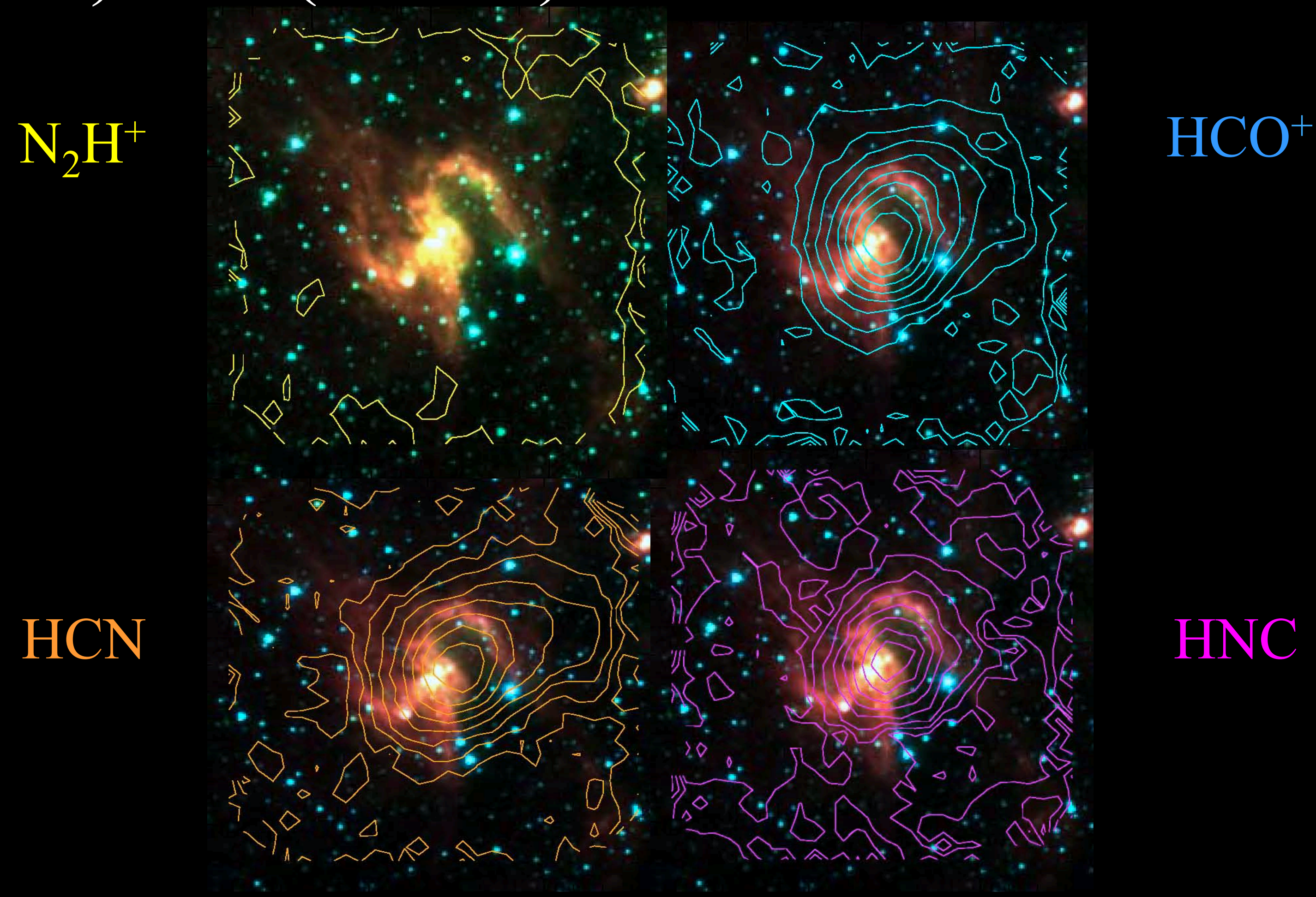

Blue - 3.6μm, Green - 4.5μm, Red – 8 μm from GLIMPSE survey

Hoq et al. 2013

A combination of N_2H^+ "only" and "drop out" morphologies

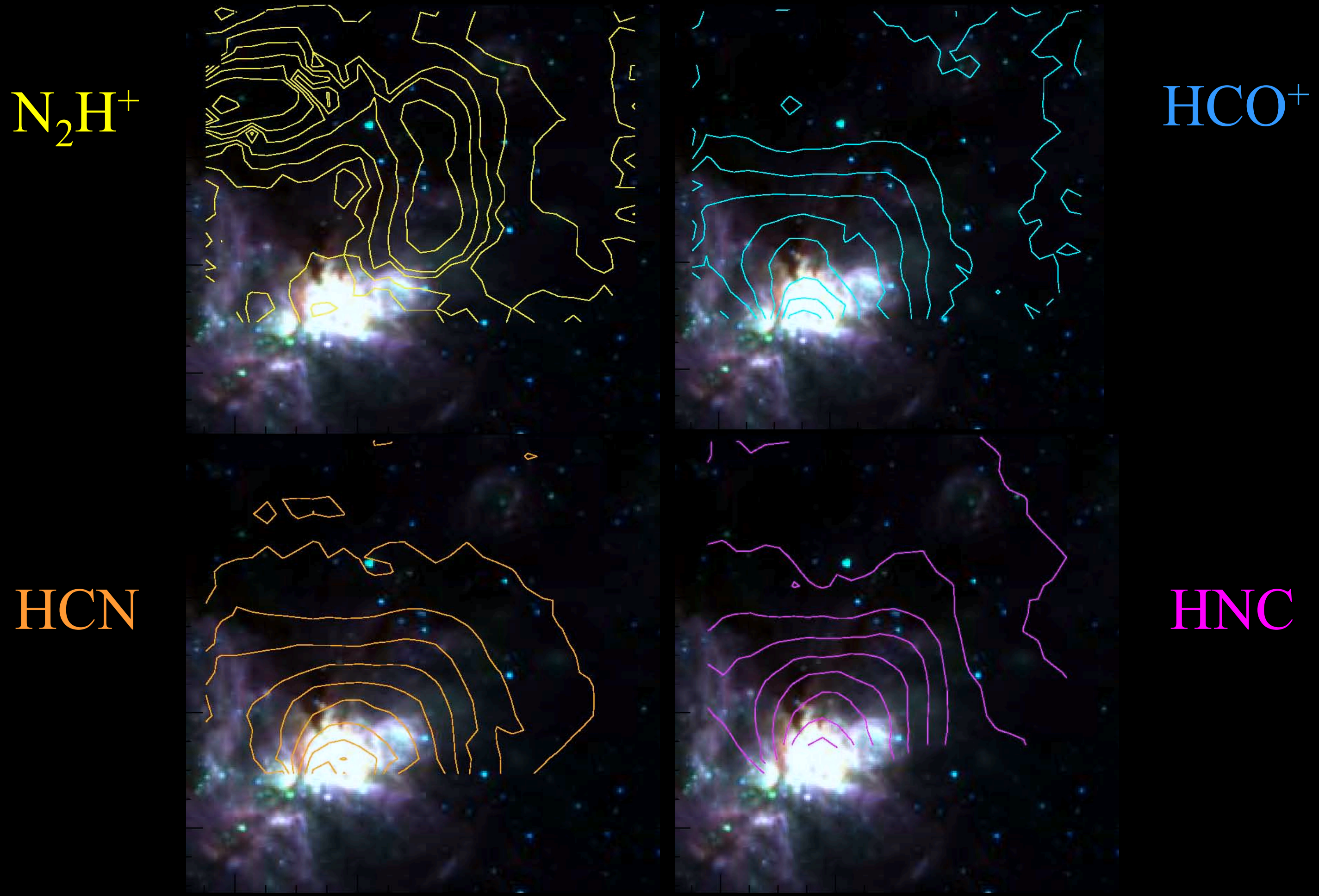

Blue - 3.6μm, Green - 4.5μm, Red – 8 μm from GLIMPSE survey

N_2H^+ poor sources are found exclusively in H II region shells

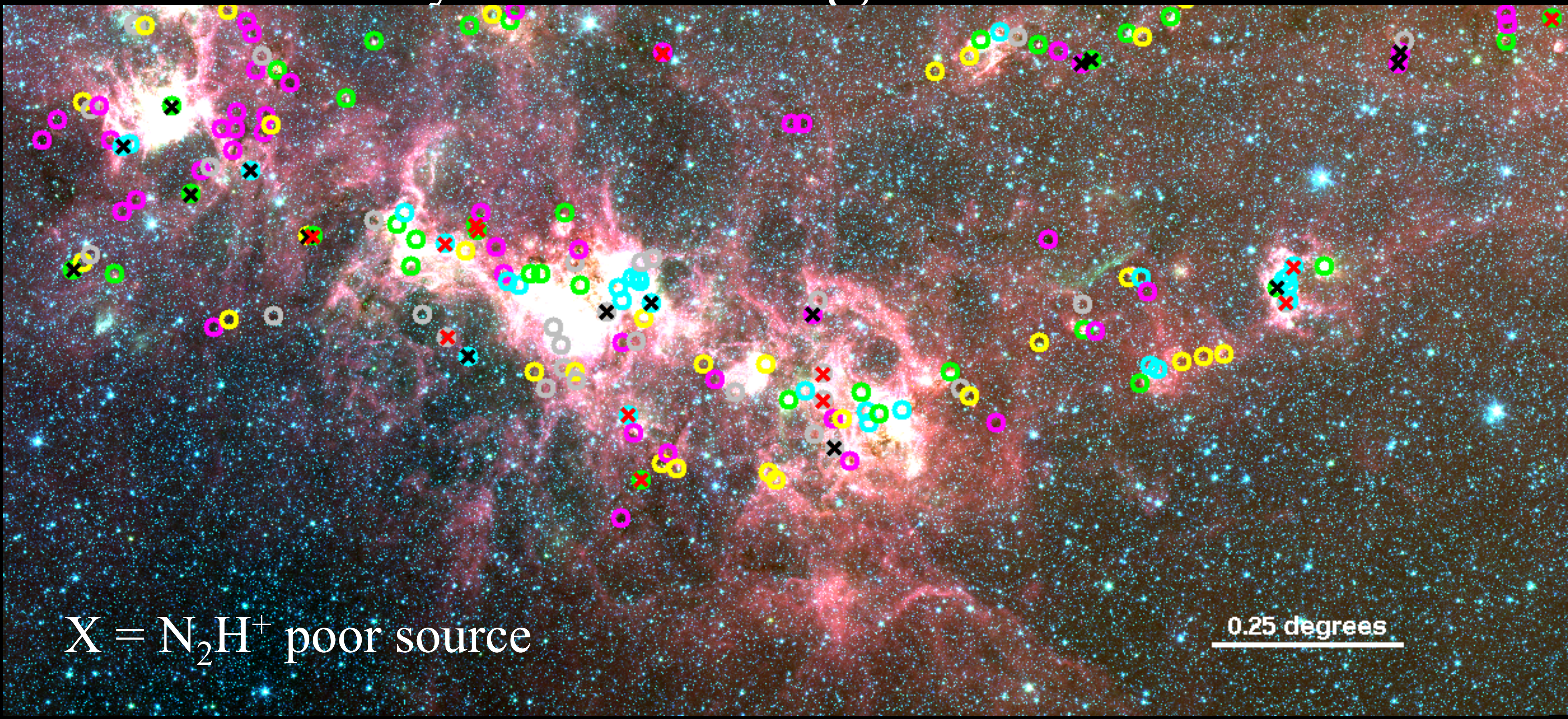

The chemistry in heated regions favors HCO+ and destroys N_2H^+

Stephens et al. 2014

The N_2H+ rich source AGAL333.234-00.062

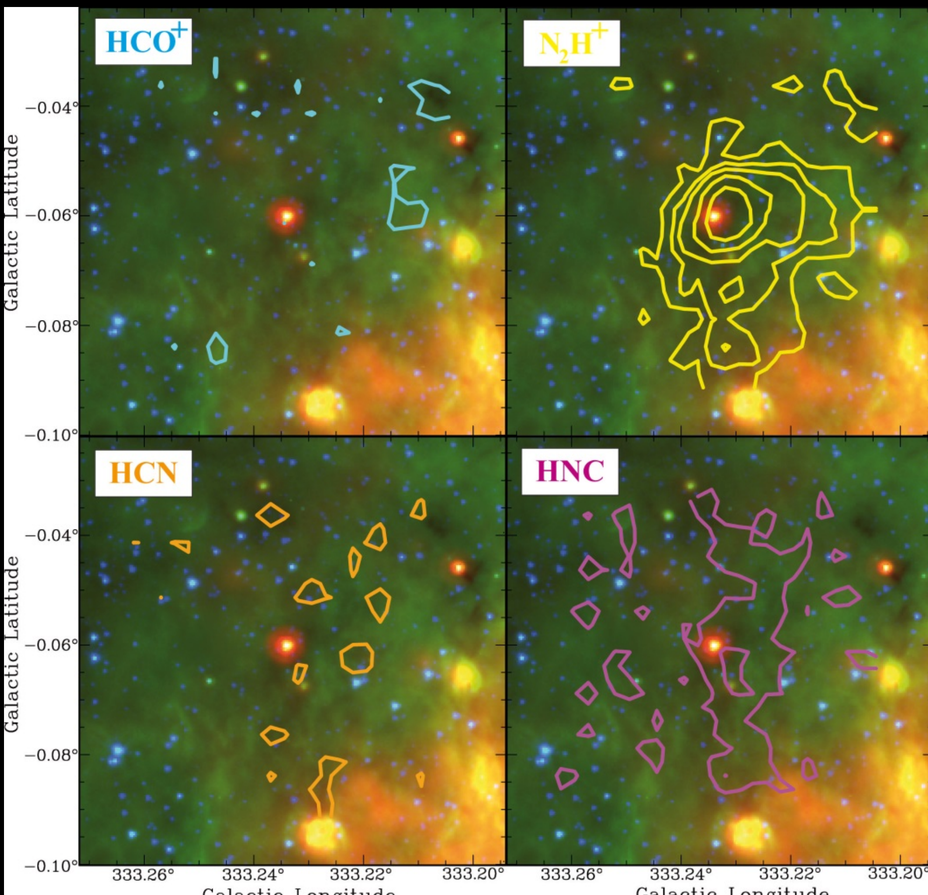

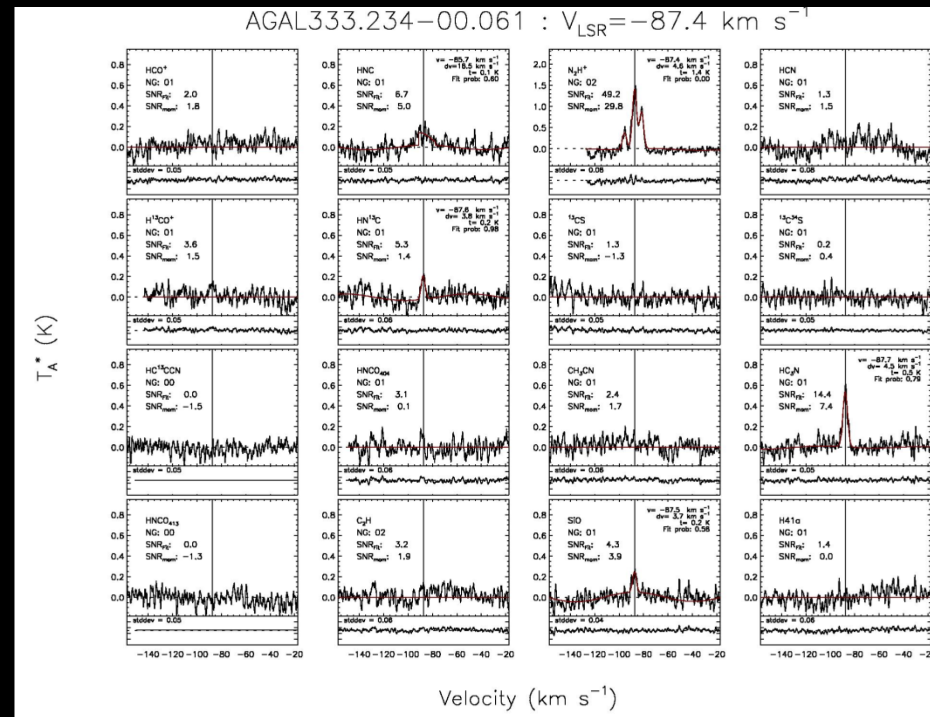

Stephens et al. 2014

90 GHz ATCA image reveals two high-mass protostars: 41 and 52 Msun

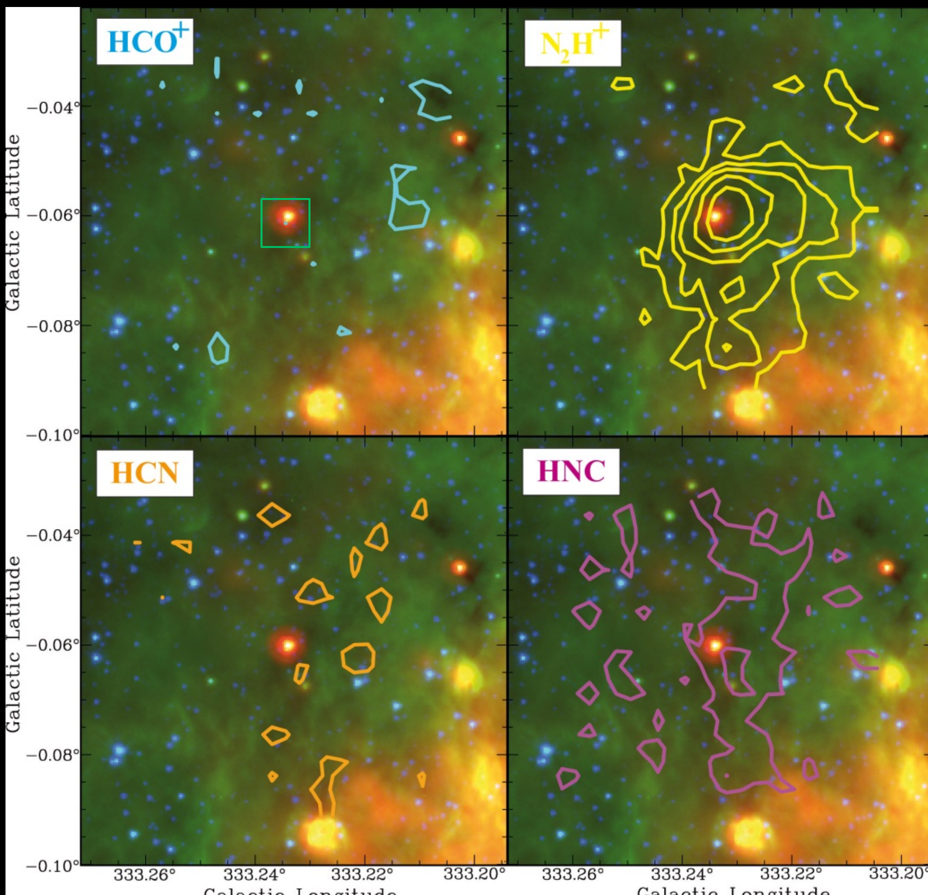

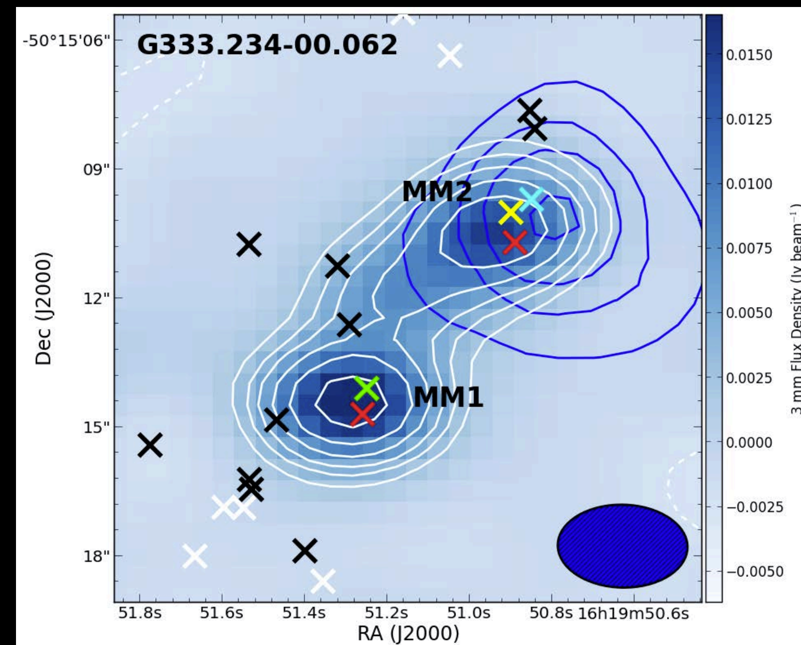

The more massive core (MM1) is in a **younger** evolutionary stage

Stephens et al. 2014

MM2 is the source of a powerful, fast outflow

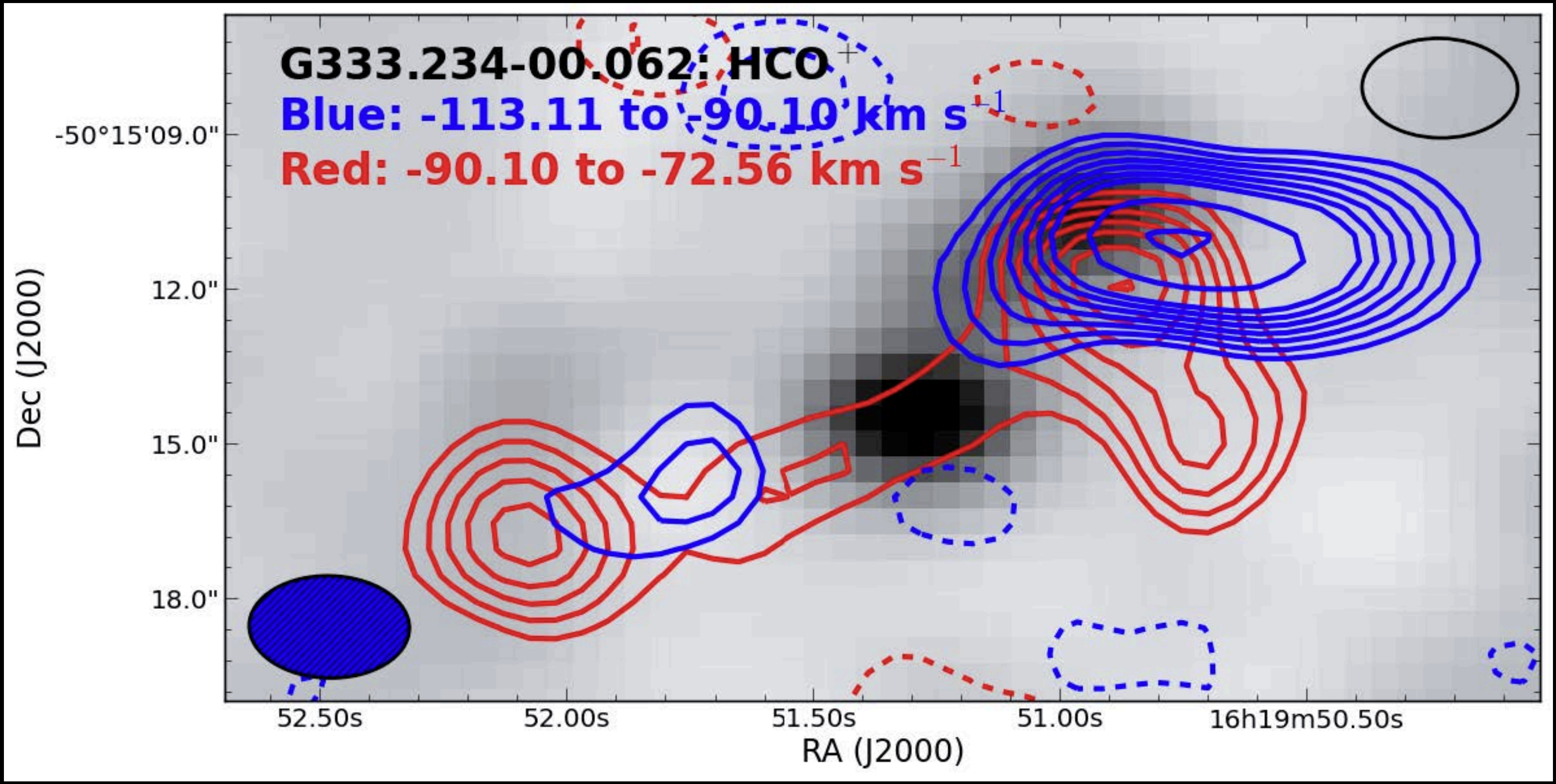

Stephens et al. 2014

The N_2H^+ "richness" is actually due to deep self-absorption of HCO^+

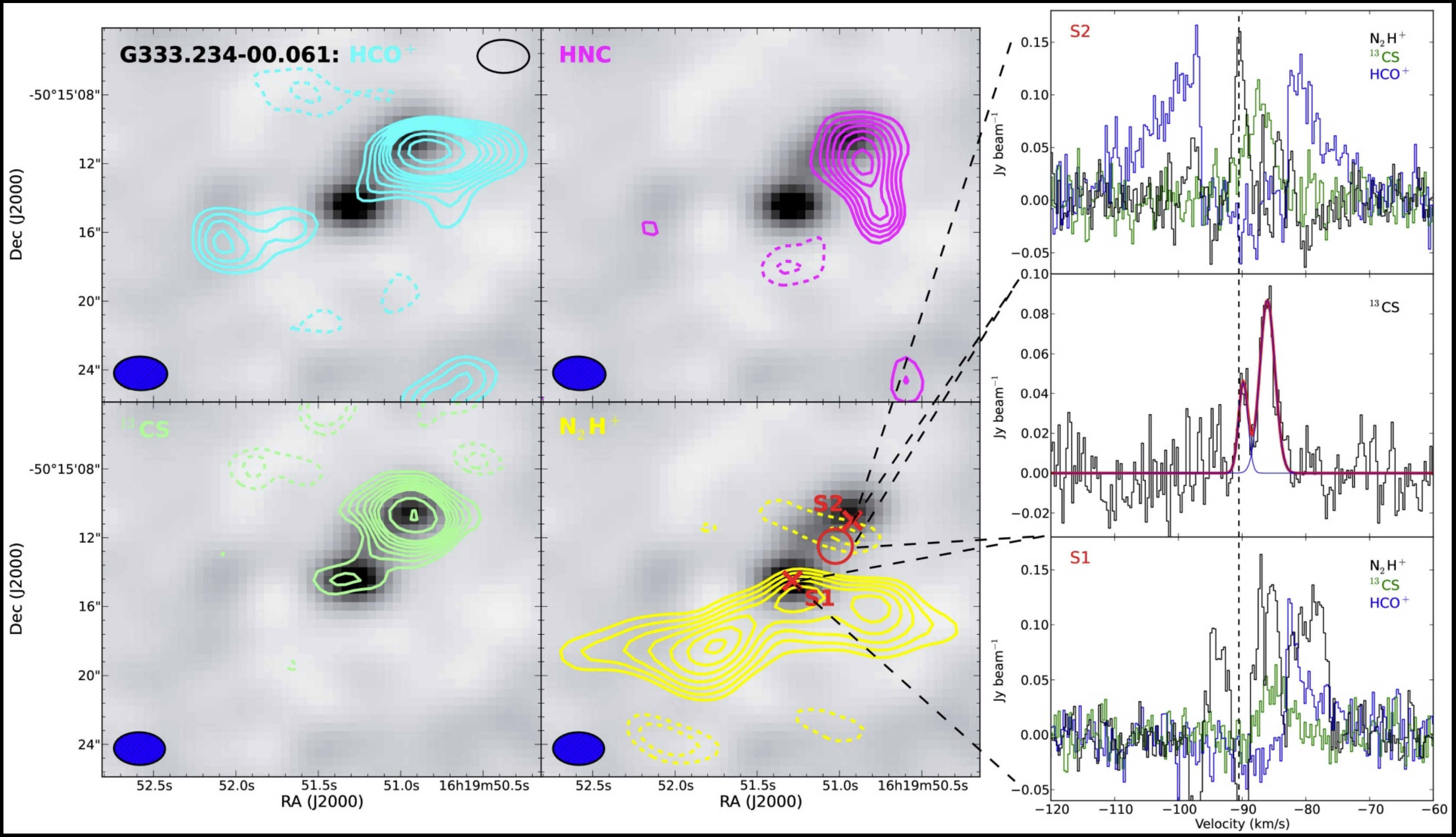

Stephens et al. 2014

The N_2H^+ "richness" is actually due to deep self-absorption of HCO+

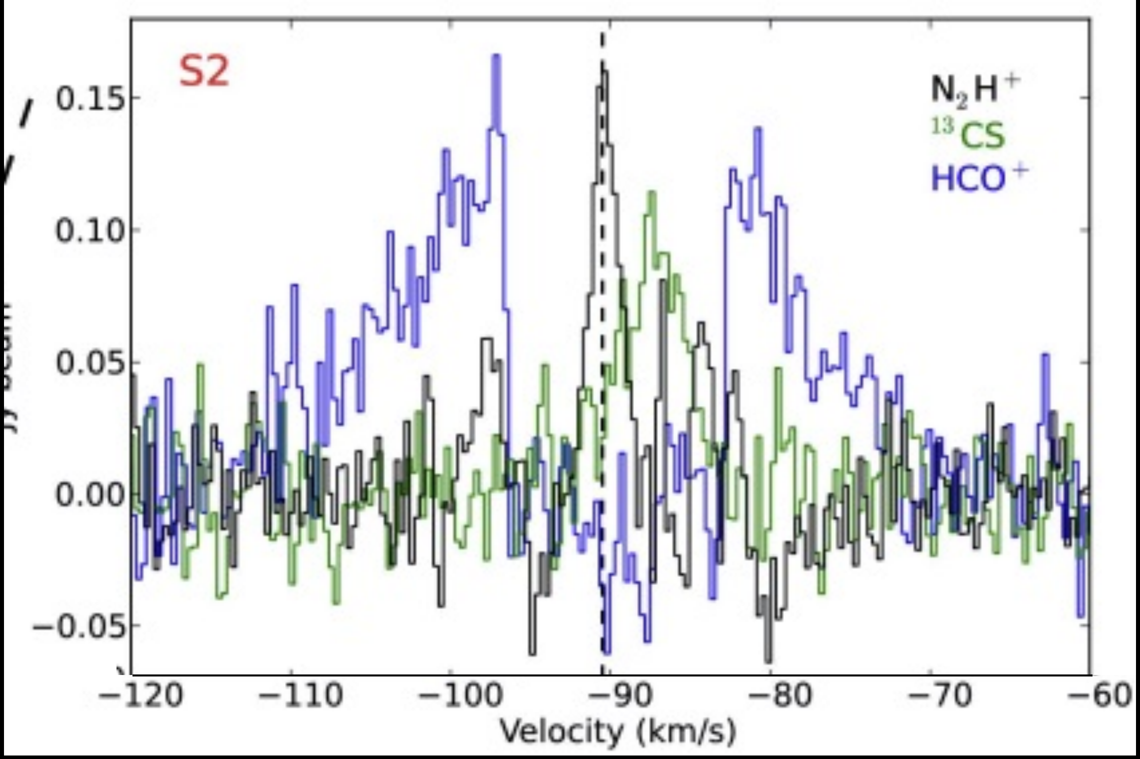

Puzzle: How can the absorbing gas, presumably cold, have linewidths of ~20 km/s? Extreme turbulence? Subthermal excitation?

Evolution: Collapse motions

- Optically thick lines with the “blue-red asymmetry” are usually interpreted as a sign of collapse.
- We use optically thick HCO+ line to search for collapse.

A collapsing cloud with a cold exterior and a warm interior

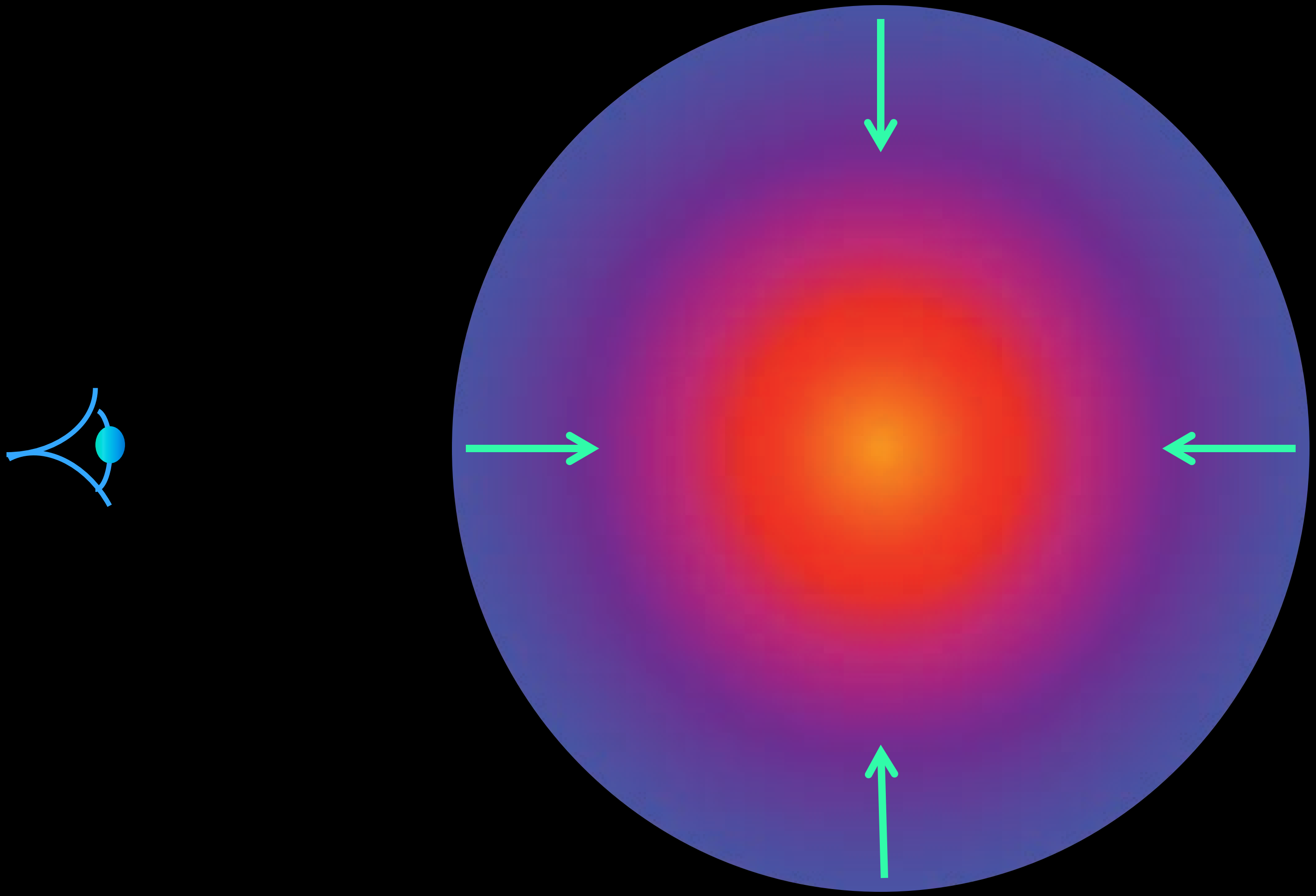

For an optically thick line, at any given velocity we see only the τ = 1 surface

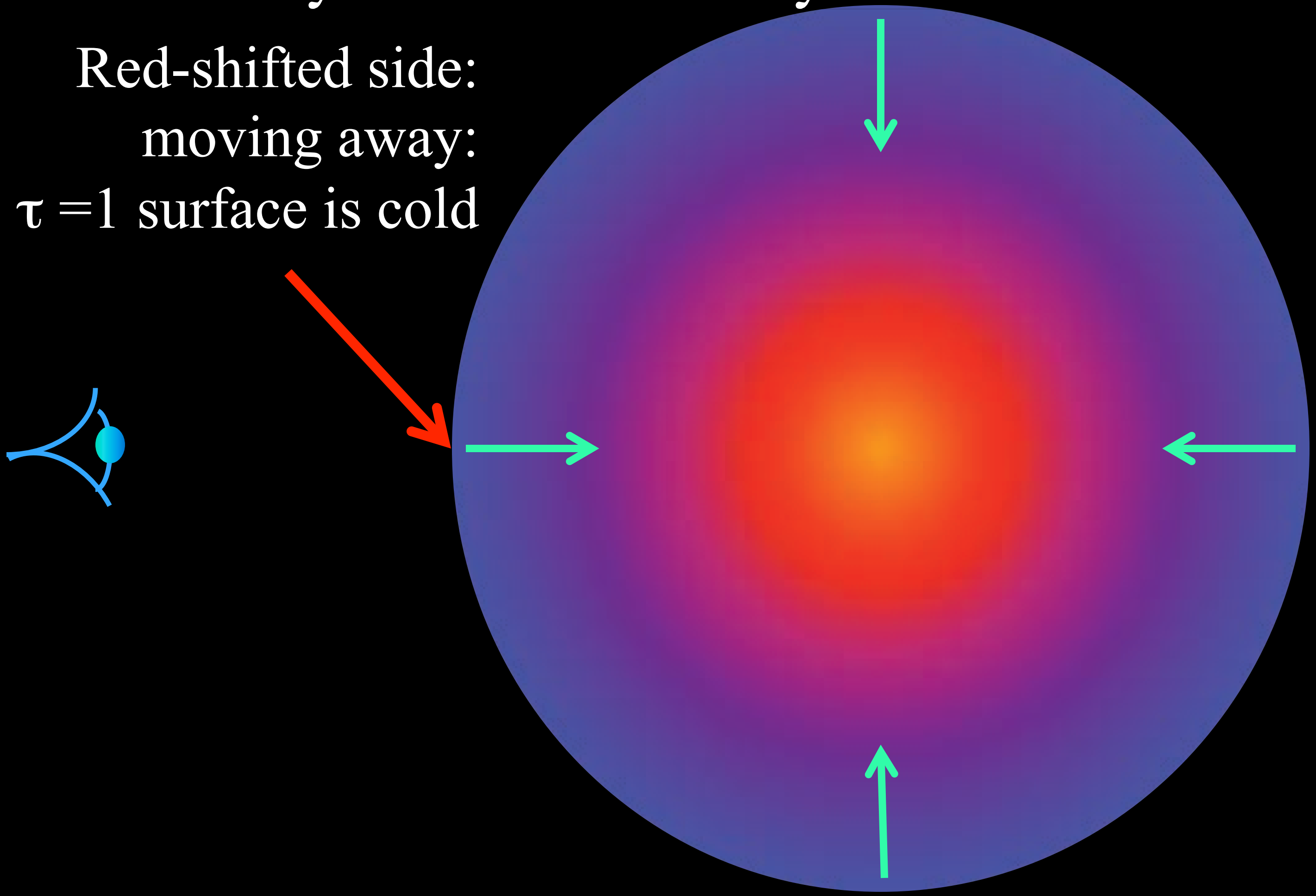

For an optically thick line, at any given velocity we see only the τ = 1 surface

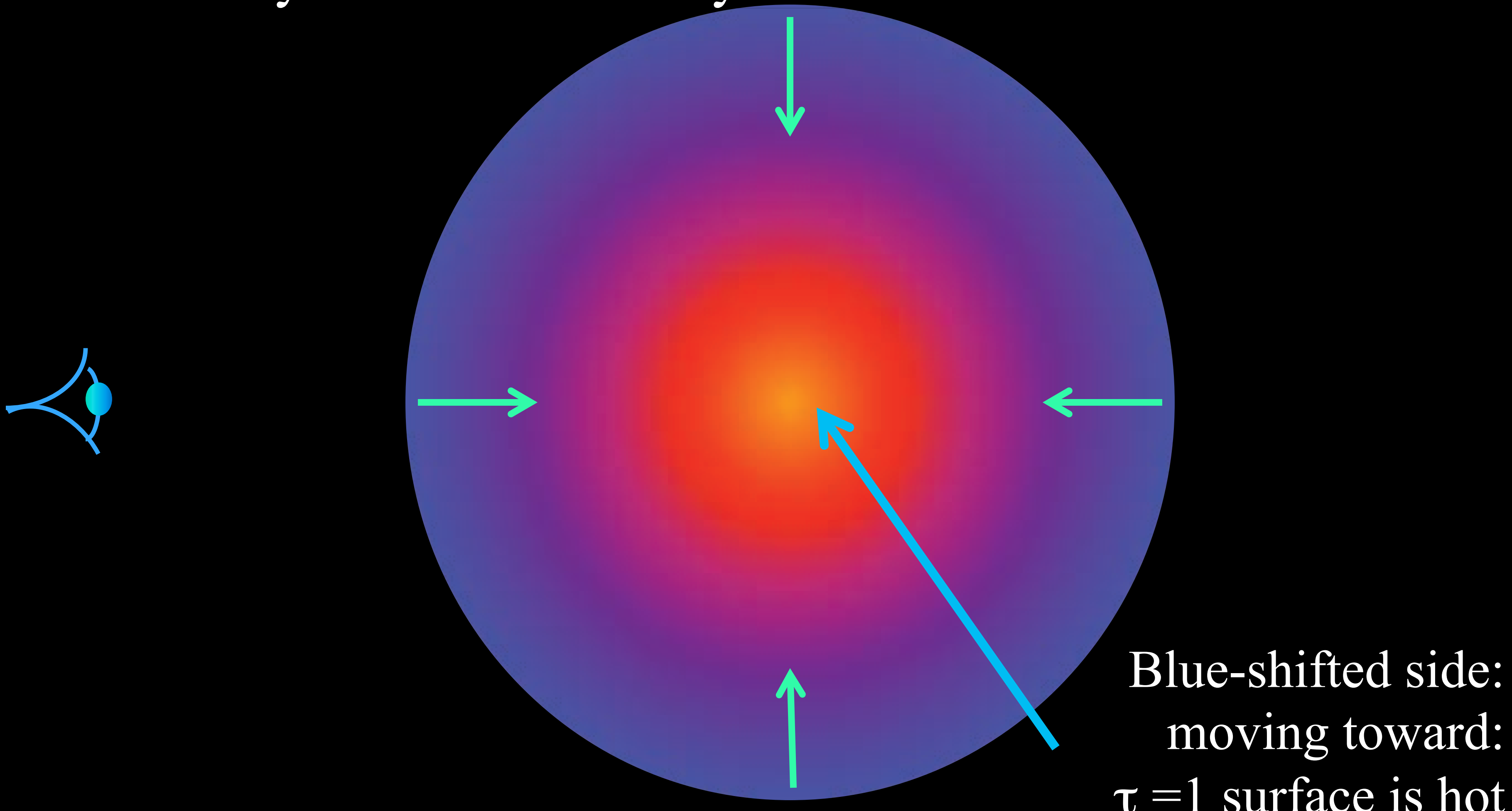

The blue-red asymmetry in a collapsing cloud with a "warm" interior

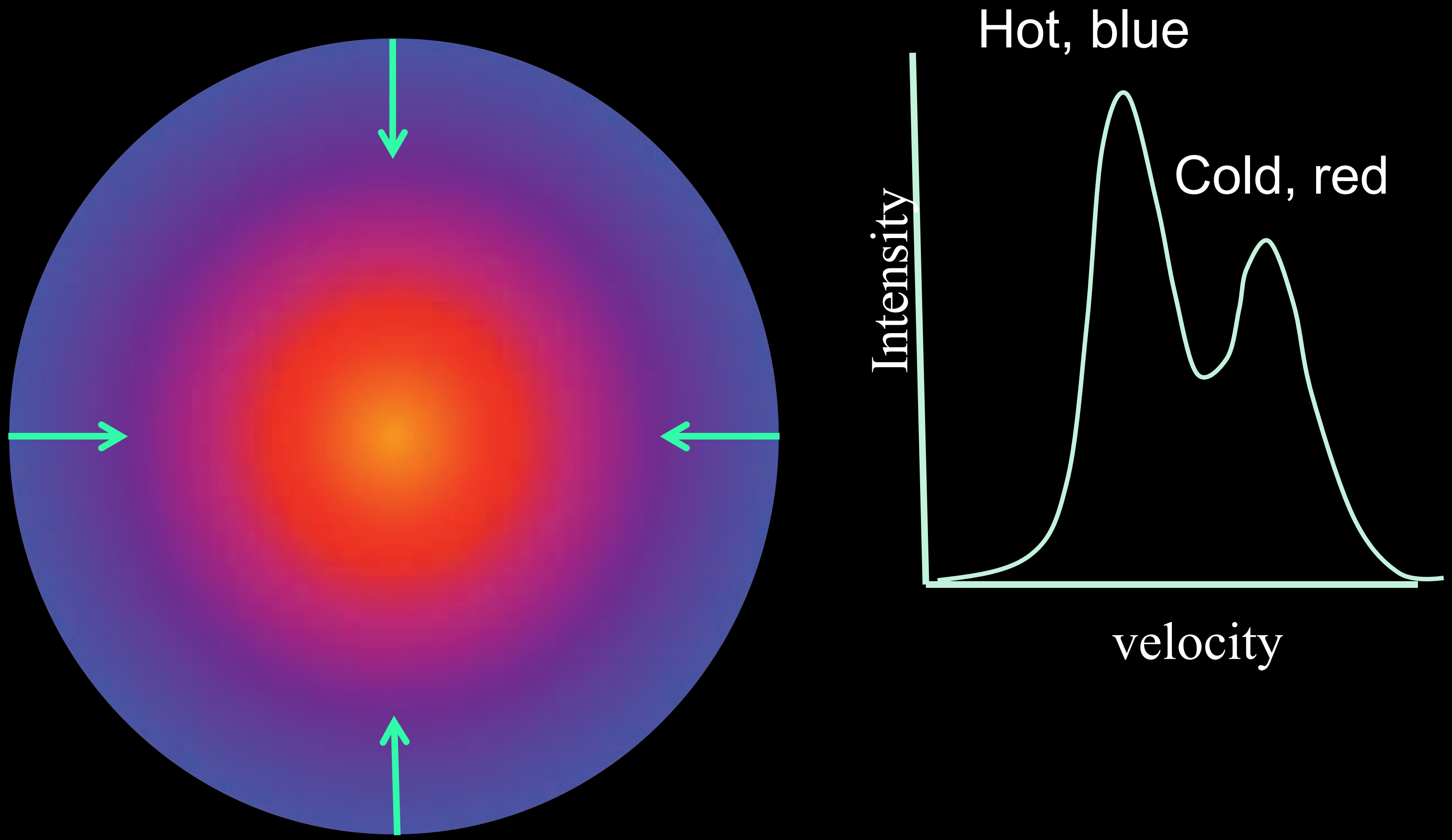

Define Asymmetry Index α

$$\alpha = \frac{I_{blue} - I_{red}}{I_{blue} + I_{red}}$$

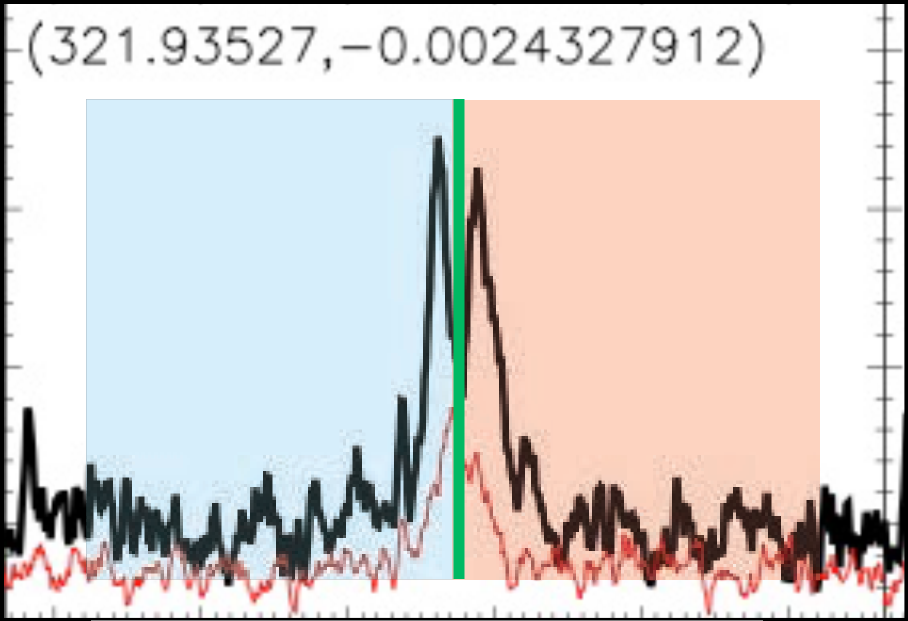

Black: HCO^+
Red: $H^{13}CO^+$

Systemic velocity from N_2H^+

Blue asymmetry $\alpha > 0$

Red asymmetry $\alpha < 0$

The ensemble of all MALT90 clumps exhibit an HCO^+ blue-red asymmetry.

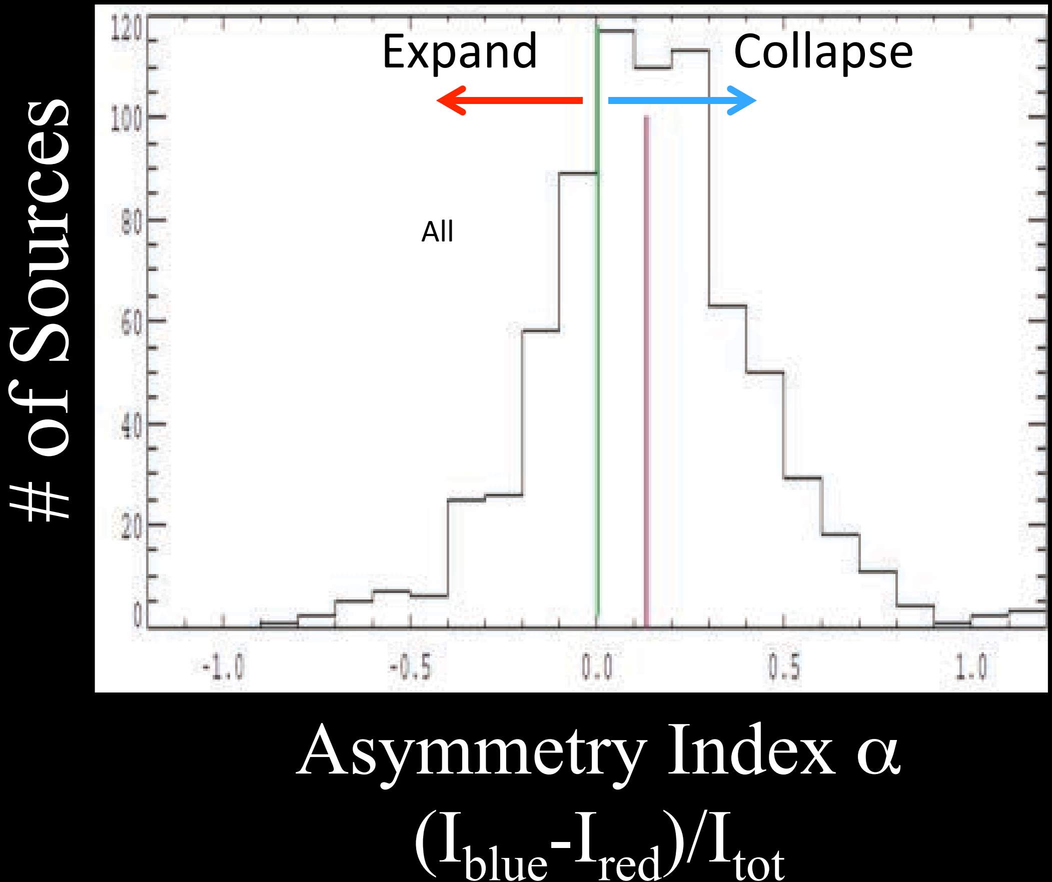

The clumps are **collapsing.**

α=0.13

Jackson et al. in prep

The blue-red asymmetry evolves

The asymmetry is largest for pre-stellar clumps and decreases steadily with evolutionary stage (protostellar, H II, and PDR)

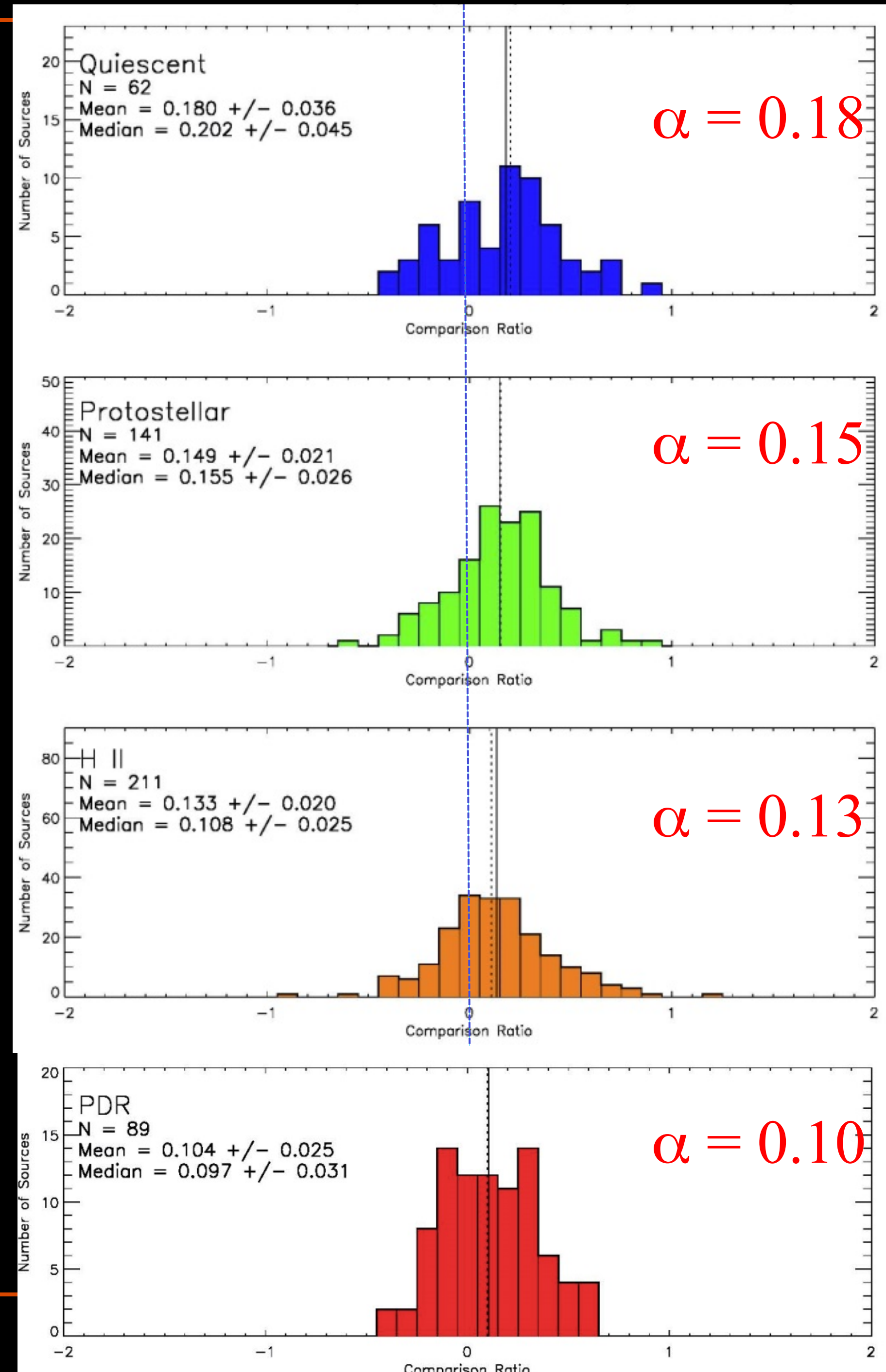

The asymmetry evolves: largest collapse motions in prestellar clumps

$V_1 - V_2$ (km/s)

$V_1 - V_2$ (km/s)

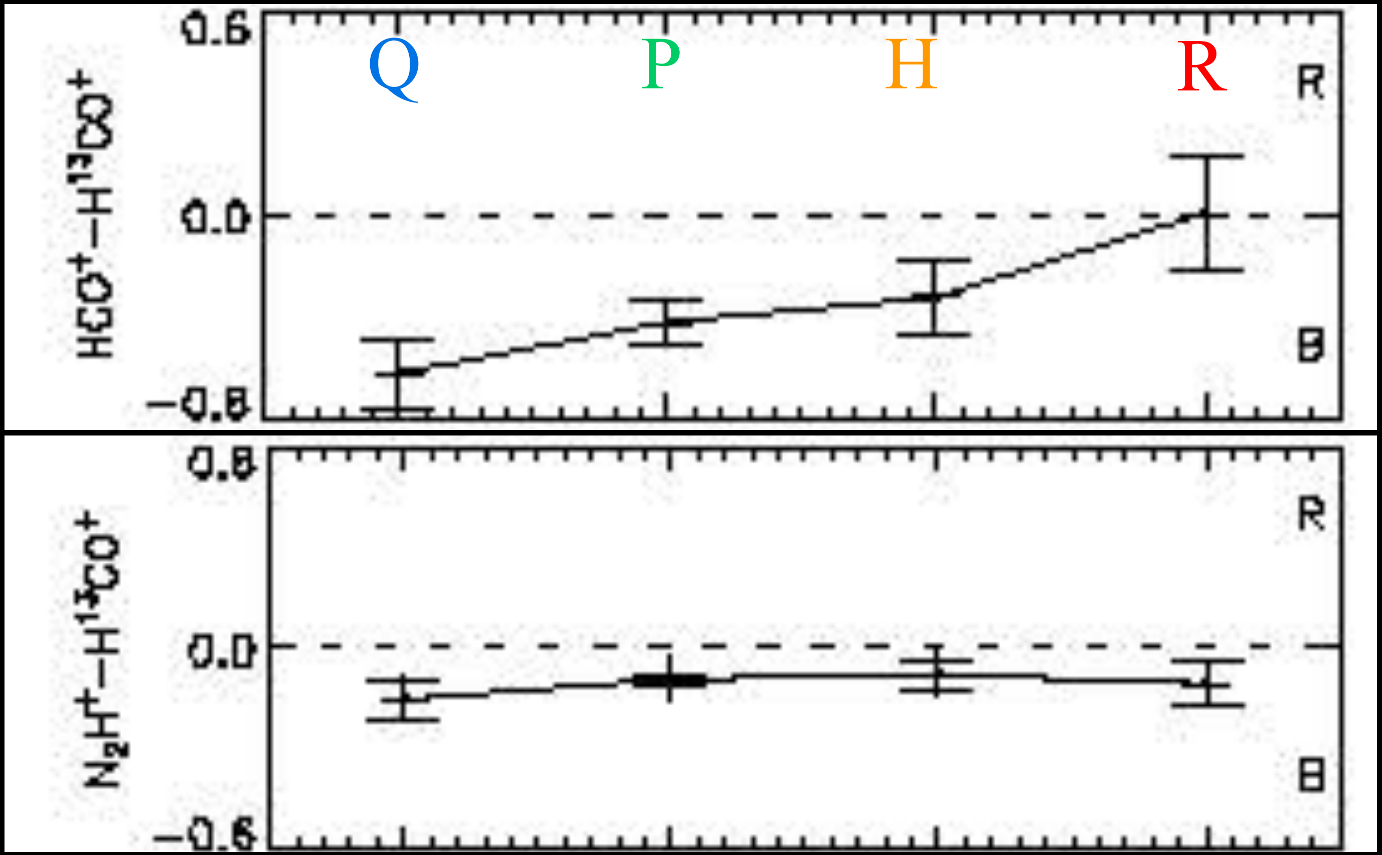

Rathborne et al. 2015

Sensible?

- Prestellar clumps---no heating source/ high temperature region
- Self-absorption occurs only if T_{ex} is subthermal ($n<n_{crit}$) in outer envelope, thermal ($n>n_{crit}$) in centre.
- $V_{inf} \sim \alpha\Delta v \sim 0.15 * 3$ km/s = 0.5 km/s
- For a M ~ 100 M_{sun} source in free-fall, the velocity $v \sim v_{inf}$ at R ~ 0.2 pc.
- In free-fall, $n \sim R^{-3/2}$. For a clump with $n_{av} \sim 10^4$ cm^{-3}, $n \sim n_{crit} \sim 10^5$ cm^{-3} at R ~ 0.2 pc.   Agrees

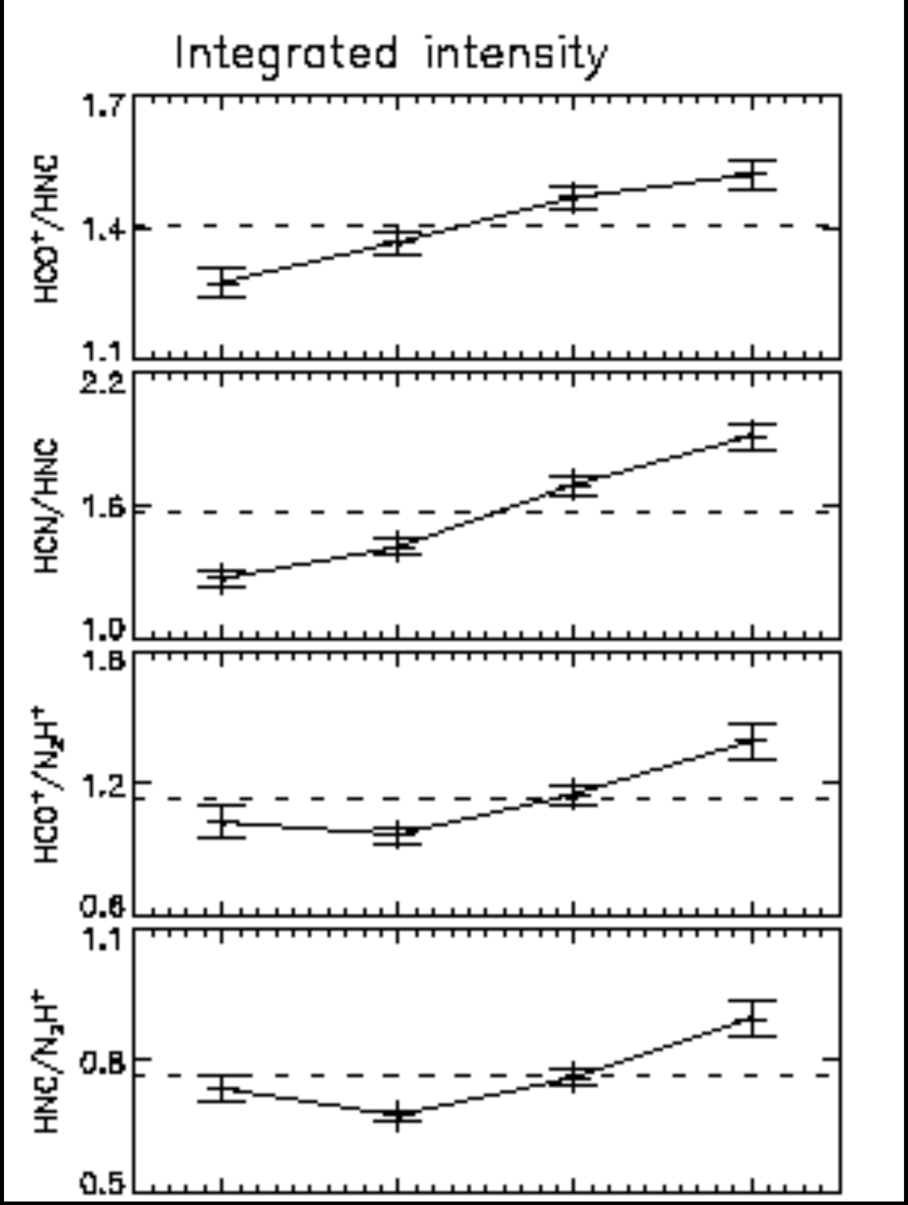

Integrated intensity
1.7
1.4
1.1
HCO+/HNC
2.2
1.6
1.0
HCN/HNC
1.8
1.2
0.6
HCO+/N2H+
1.1
0.8
0.5
HNC/N2H+

Evolution: Maser activity
The clumps are associated with masers

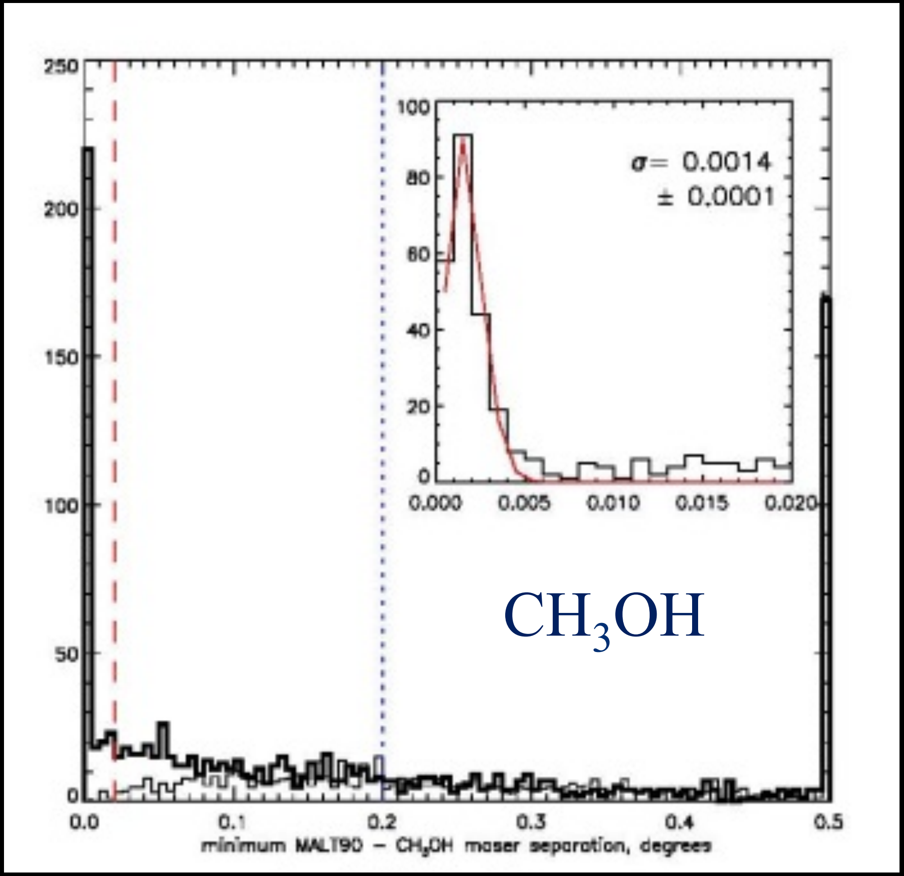

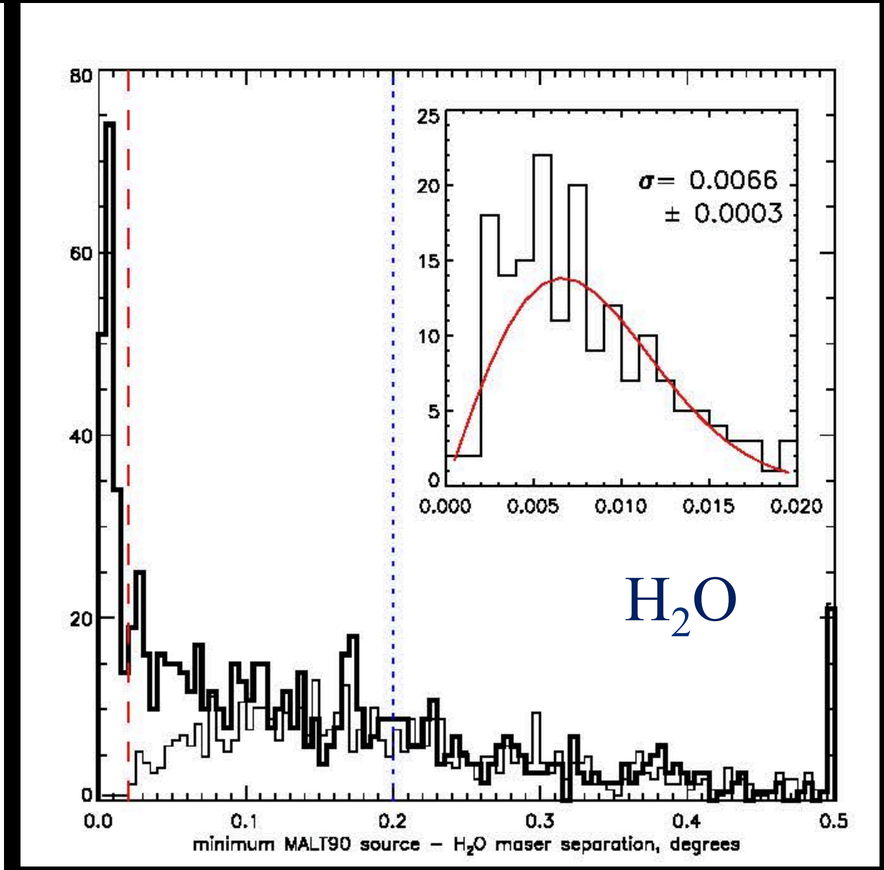

Distance to nearest maser: MMB and HOPS

Breen et al. 2012a,b; Walsh et al. 2014;Jackson et al. in prep

L-V Diagram MALT 90/MMB/HOPS

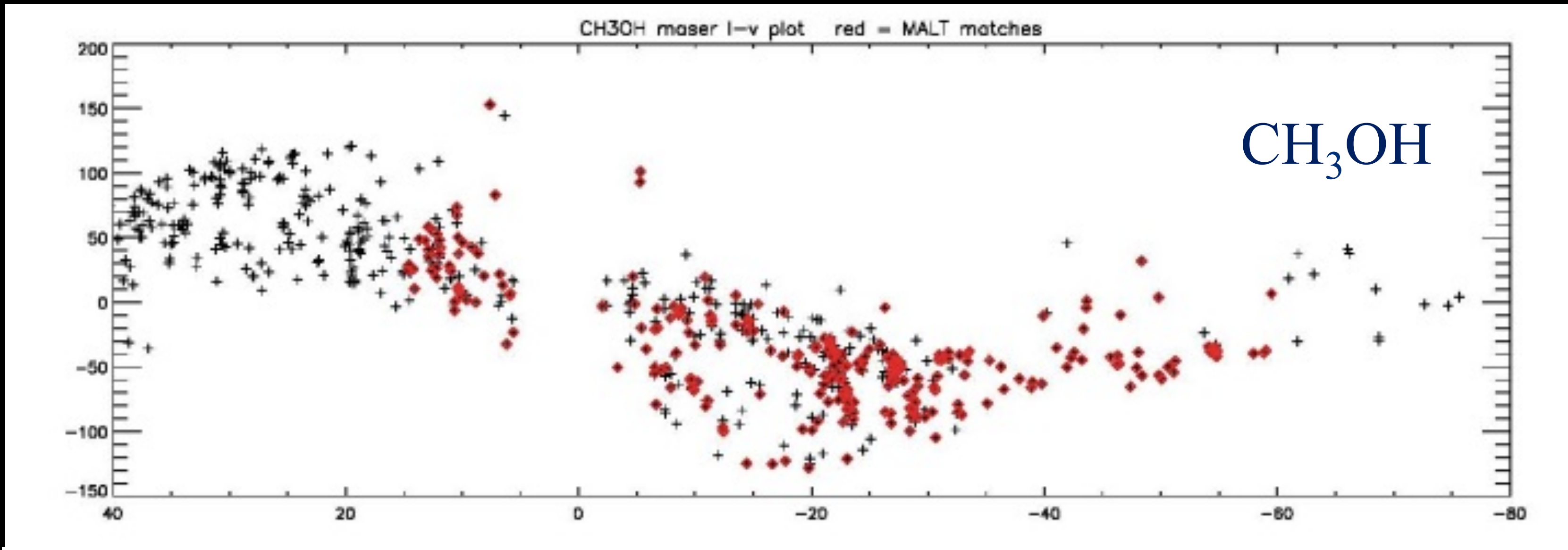

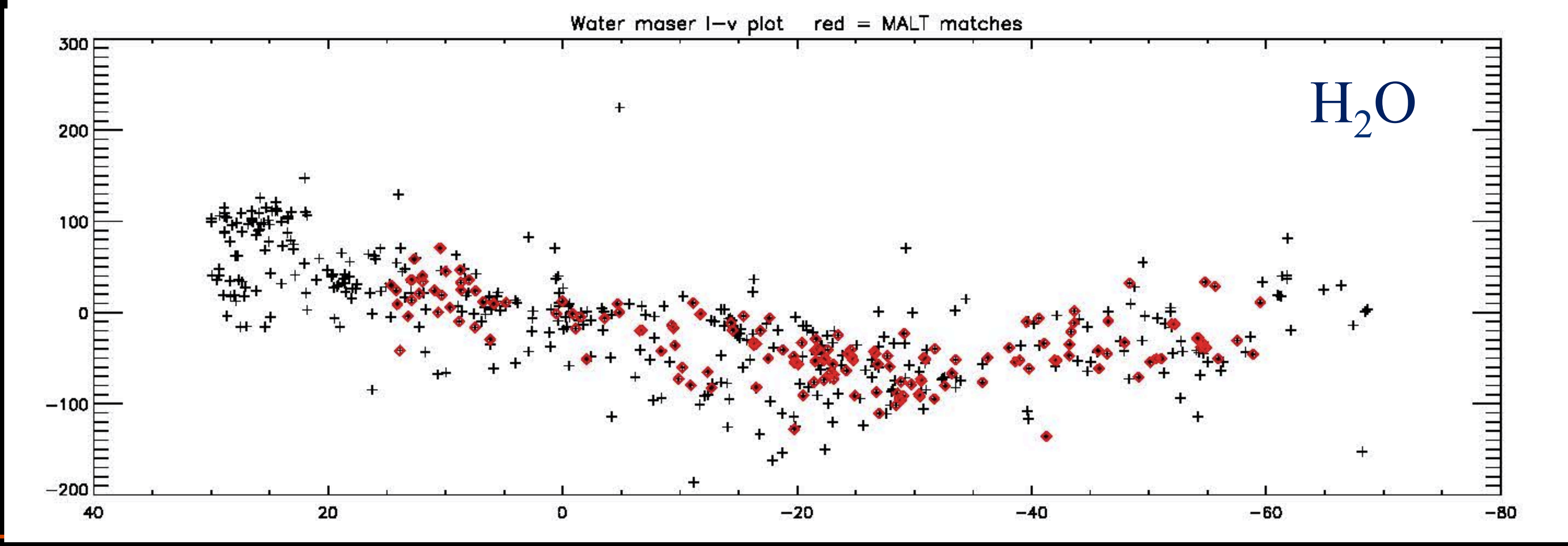

The MALT90 velocity and methanol maser velocities match

The MALT 90 velocities match the methanol maser velocities. MALT 90 sources are high-mass star-forming regions.

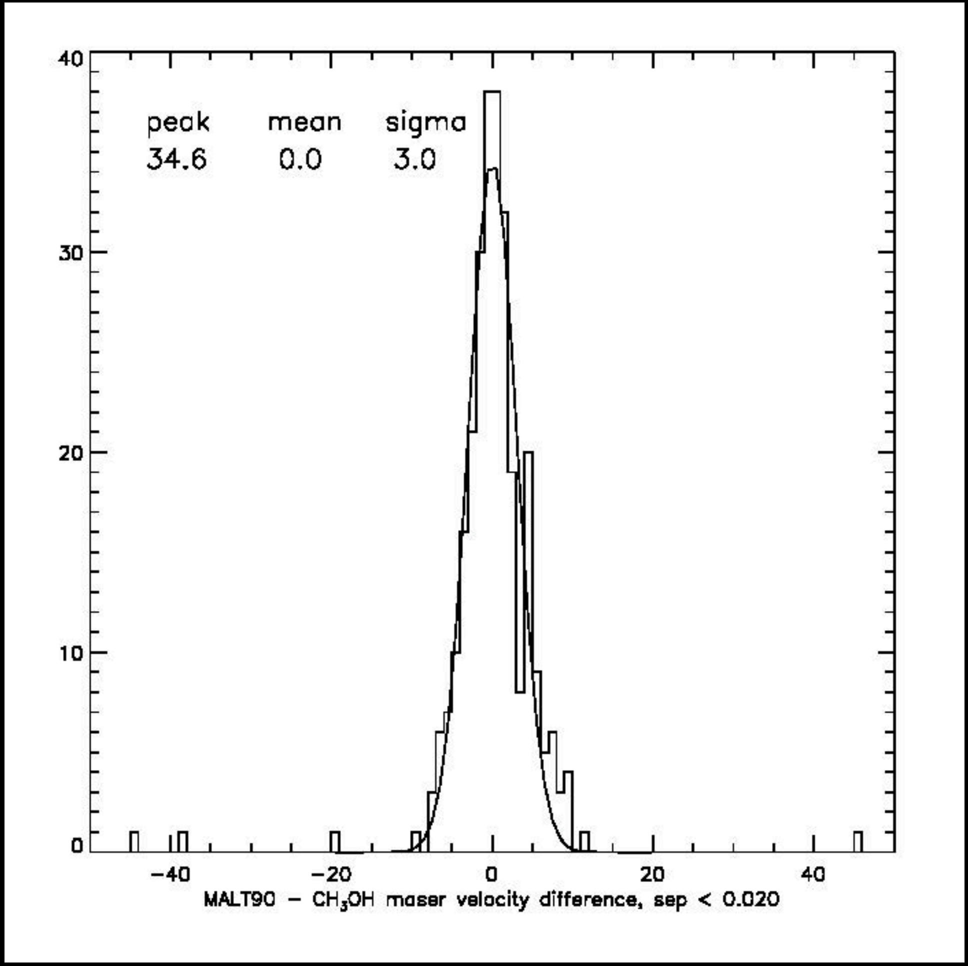

Jackson et al. in prep

The maser activity evolves: Peaks in protostellar and H II region phases

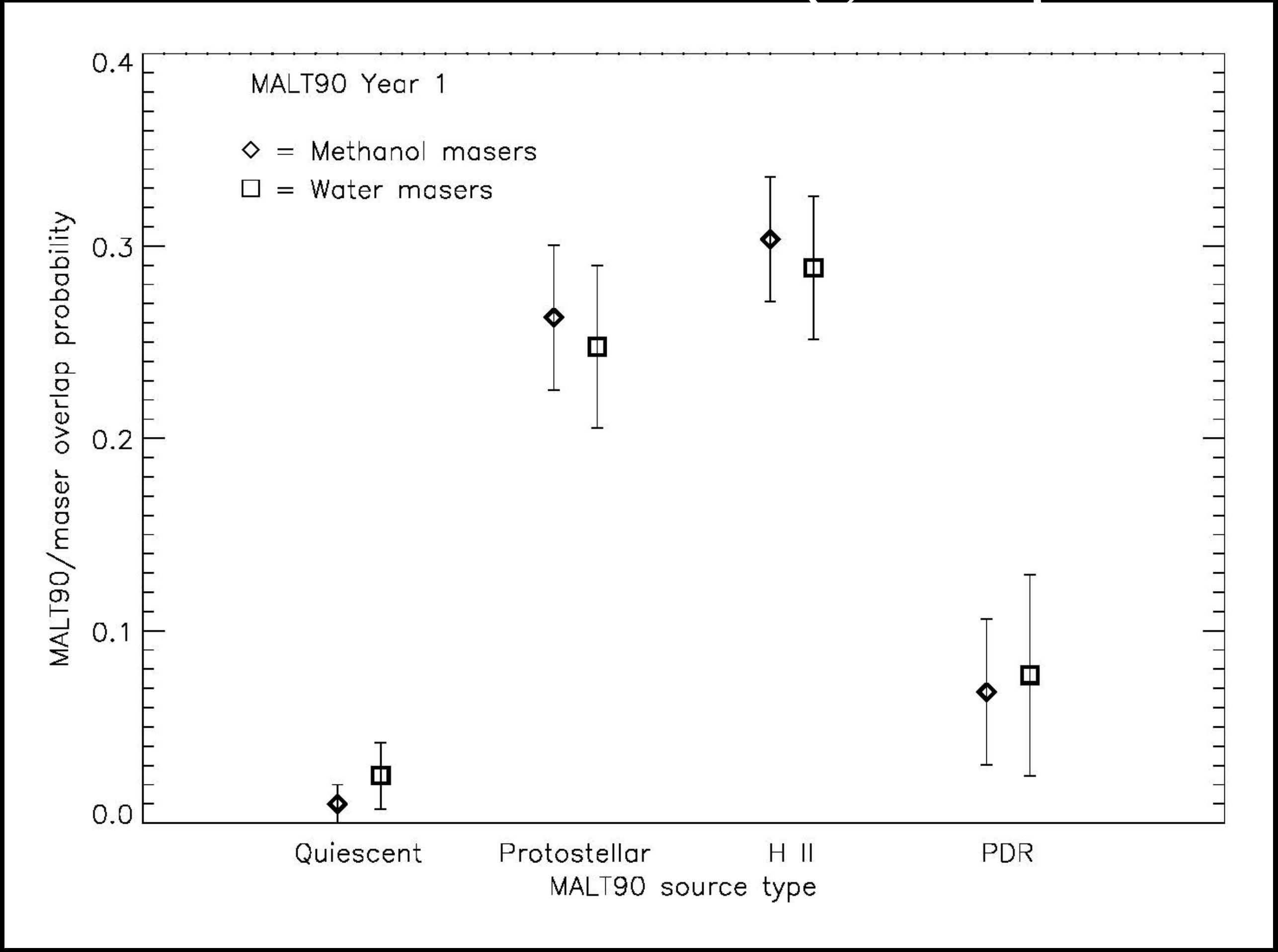

Jackson et al. in prep

Evolution: Summary

As clumps evolve from pre-stellar, to protostellar, to H II regions

- Temperature increases monotonically
- Chemistry changes: N_2H^+ poor sources at late times. N_2H^+ rich sources at pre-protostellar phases due to self-absorption.
- Collapse motions decrease monotonically
- Maser activity peaks in the protostellar and H II region phases

The gas content-star formation rate relation in galaxies

- The Schmidt Law correlates gas surface density with star formation rate
- Another representation of this relation compares the molecular gas mass content (traced by molecular line luminosity, typically HCN) vs. star formation rate (traced by far-infrared luminosity) for entire galaxies. (Gao & Solomon 2004).

Molecular gas vs FIR luminosities

- The correlation works well for CO vs. FIR.
- The correlation works much better for HCN vs. FIR (Gao & Solomon 2004).
- Interpretation: only the dense gas content really matters, and there is a roughly constant efficiency in converting dense gas to stars.
- Dense gas traced by HCN, star formation traced by FIR.

The HCN-FIR Relation

What is the basis for this relationship?

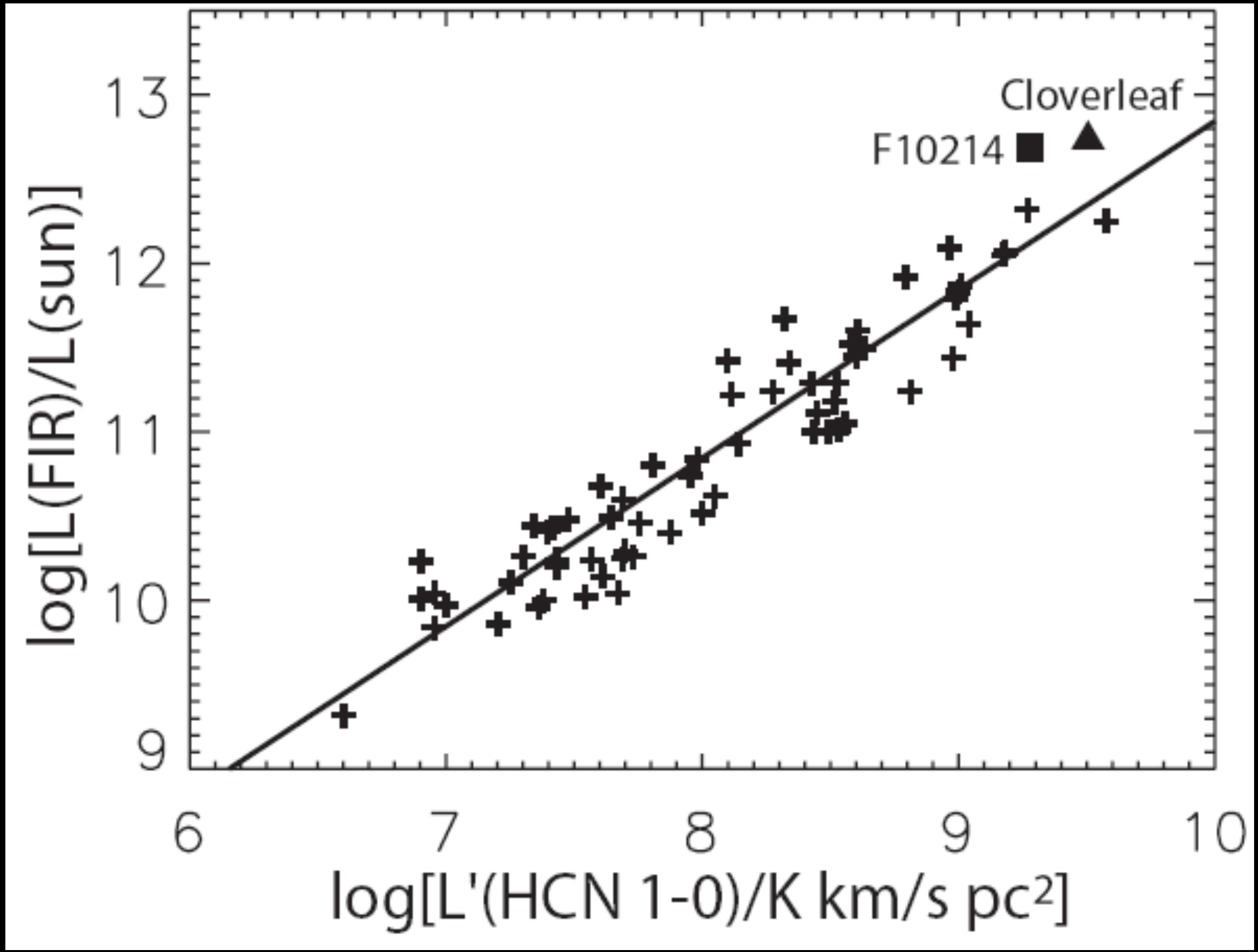

Investigate the relationship between FIR and HCN luminosity for clumps

- MALT 90 supplied kinematic distances.
- Because MALT90 mapped the clumps, we can determine the HCN luminosity robustly.
- Estimate far IR luminosities from IRAS fluxes (and MALT90 distances) in exactly the same way as for galaxies.

The HCN-FIR luminosity correlation

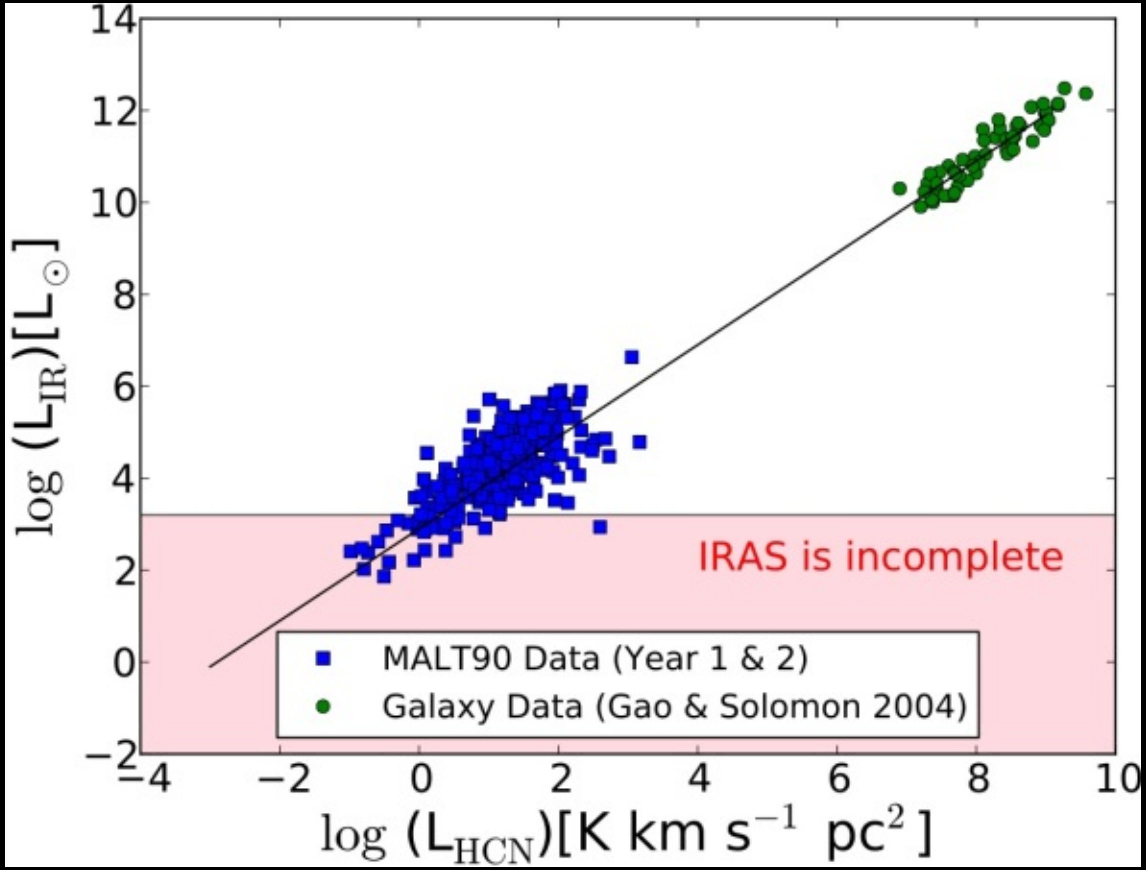

The relationship for galaxies arises from averaging a large number of clumps in the telescope beam.

Jackson et al. 2013, see also Wu et al. 2005

HCN-FIR relationship holds for clumps

- The basic unit of star formation is the dense clump
- The clumps have a ~constant HCN/FIR luminosity ratio (~star formation efficiency)
- The Gao & Solomon (2004) relationship for galaxies simply results from counting the number of these clumps in a galaxy.

The L_{dust}/L_{HCN} ratio evolves

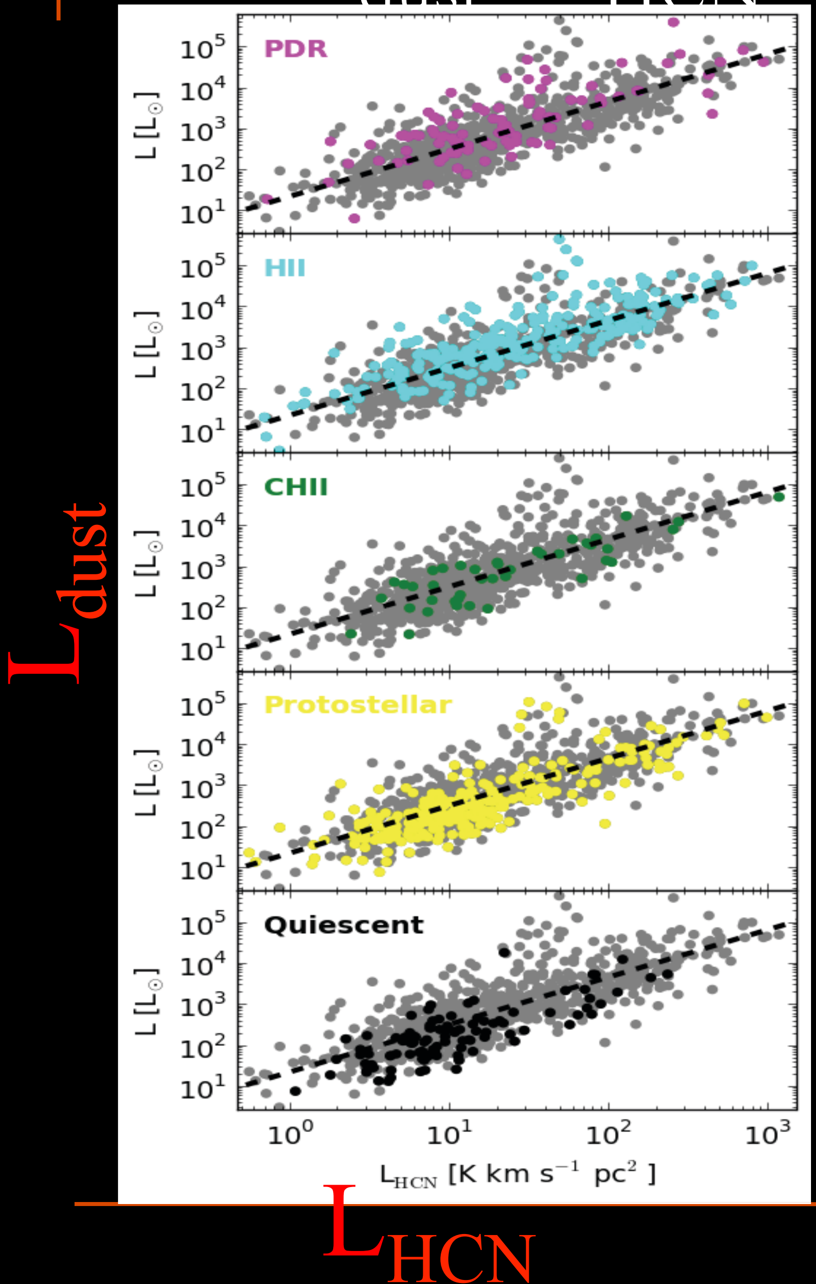

Use *Herschel* to measure L_{dust}. The L_{dust}/L_{HCN} ratio increases with time (as the stars form and generate more luminosity).

(Contreras, Guzman, Stephens)

G0.25+0.16: the most massive cold non-star forming cloud

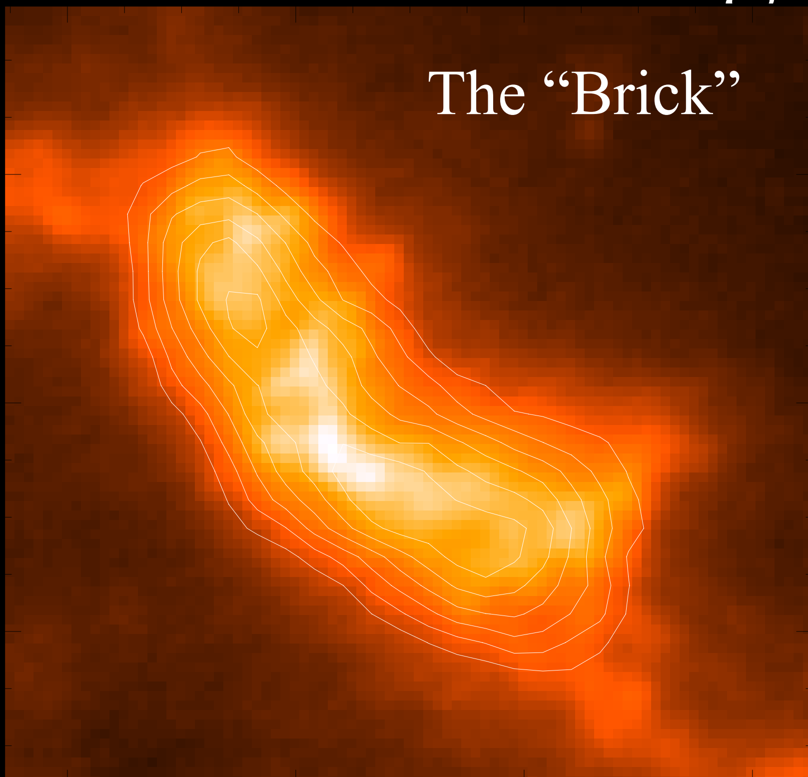

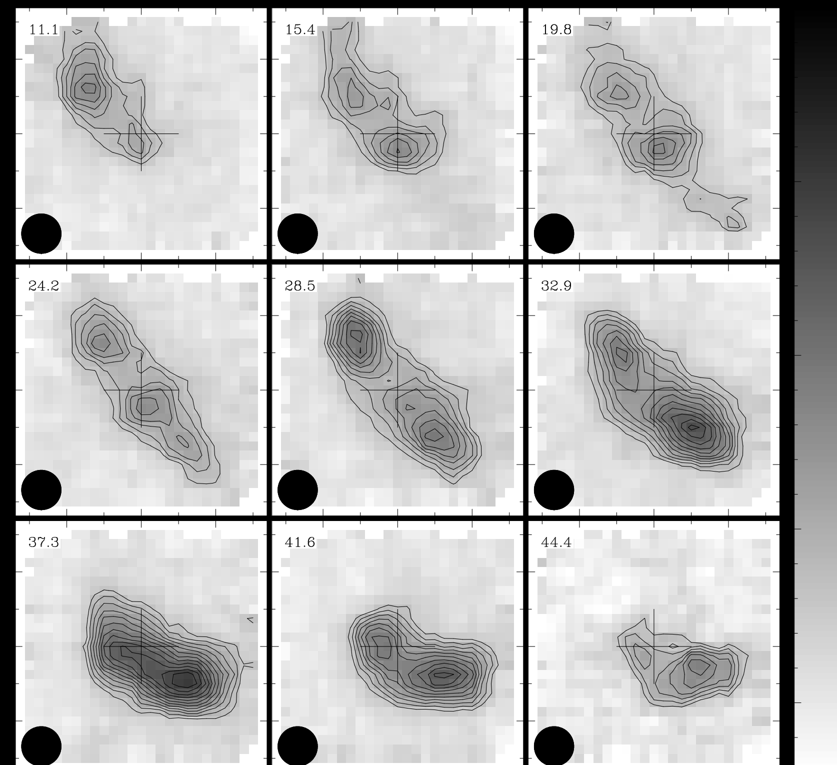

JCMT 450 µm (image, 0.3pc), MALT90 dense gas (contours, channel maps, 1.2pc)

We need better angular resolution to resolve cores

Blue - 3.6µm, Green - 8µm, Red - 24µm

Rathborne et al. 2013

Summary

- MALT 90 has mapped 2,014 high-mass star-forming clumps.
- They are located in spiral arms.
- The clumps show significant evolution in their collapse motions and maser activity.
- The Gao-Solomon HCN-FIR luminosity relation in galaxies stems from individual clump properties.
- MALT90 will be a prime finding chart for ALMA.